Image deblurring

Loïc Denis
a joint work with Eric Thiébaut, Ferréol Soulez
and the other members of ANR MiTiV

Workshop SIERRA: Signal-Image en Région Rhône-Alpes

Sept 2013

Before starting...

Short presentation of our research group:

ANR MiTiV: Méthodes Inverses pour le Traitement en Imagerie du Vivant

Multidisciplinary group lead by Eric Thiébaut (Observatoire de Lyon), gathering people from:

- astronomy (Observatoire de Lyon + Institut d'Astrophysique de Paris),

- image processing (Laboratoire Hubert Curien à St Etienne, CPE Lyon, TIMC-IMAG),

- bio-medical imaging (Centre Commun de Quantimétrie de Lyon 1, Hôpital de la Croix Rousse),

- software development (Shaktiware).

Before starting…

Illustration of the problems considered:

gated | compensation (2 “scans”)

Rit *et al.*

thèse de Fabien Momey (1 seul “scan”)

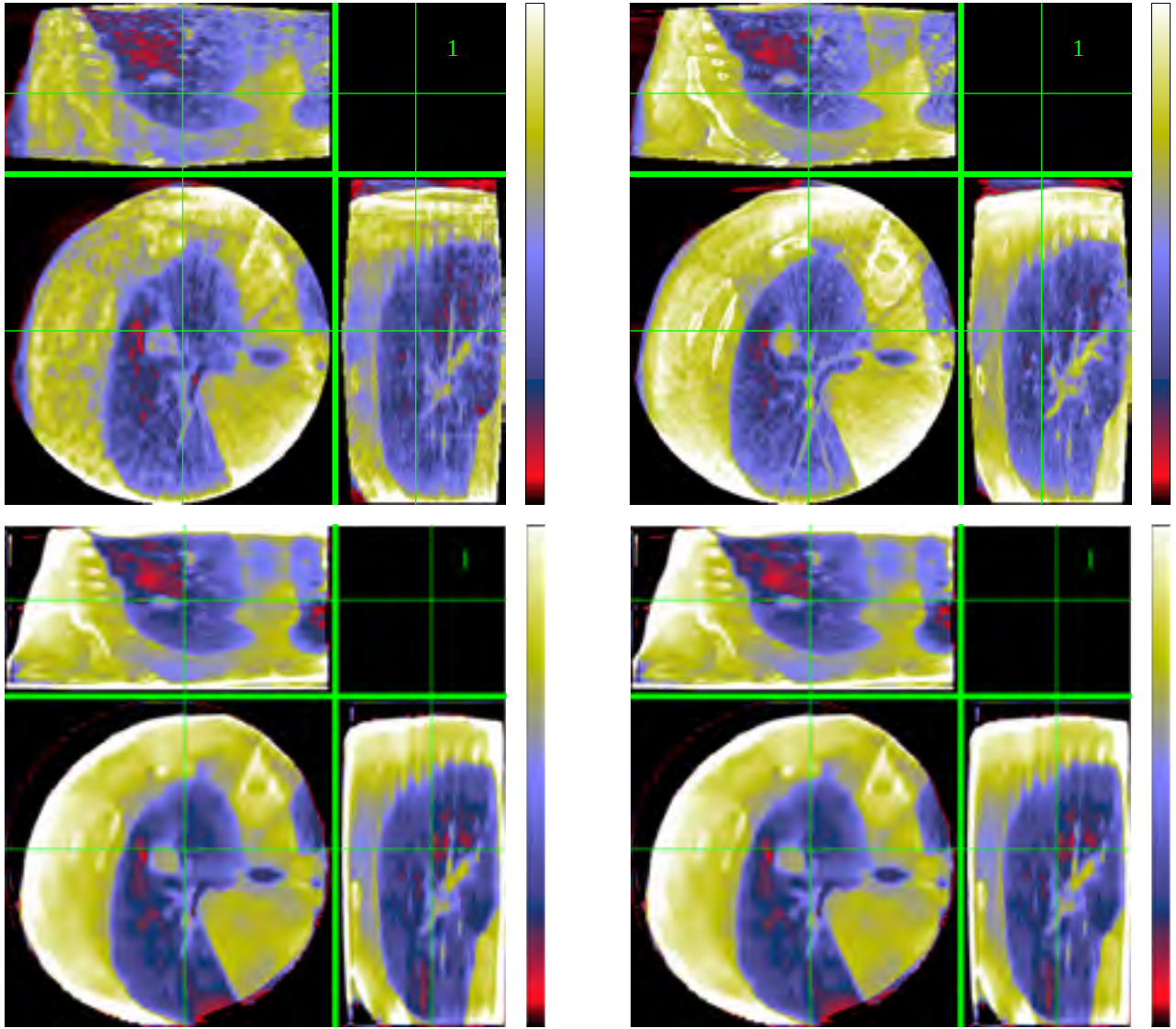

Topics of my talk:

1. An introduction to image restoration
2. Models and inversion of shift-variant blur
3. Blind deconvolution in 3D microscopy

Why digitally restore images?

→ to reduce noise

→ to improve resolution of blurred images

→ to improve the contrast of blurred structures

→ to fake a higher resolution:

from “Example-based super-resolution”, Freeman *et al.*, 2002.

Denoising *vs* Deblurring

Denoising: when the most significant part of the degradation comes from noise (little blur)

$\rightarrow$ some smoothing is unavoidable

Deblurring: when blur is stronger and the signal-to-noise ratio is high enough to improve the resolution

$\rightarrow$ special care must be paid to prevent from noise amplification

Denoising and deblurring methodologies have long been very close: Wiener filter, Markov random fields, total variation minimization, wavelets methods. . . .
During last decade, denoising approaches have significantly differed: role played by image patches (selection-based estimation, redundancy of image patches, patch dictionaries). The methodological gap with deblurring methods is still to be filled. . .

The 3 ingredients of a deblurring method

1. The degradation model 1/2: blur

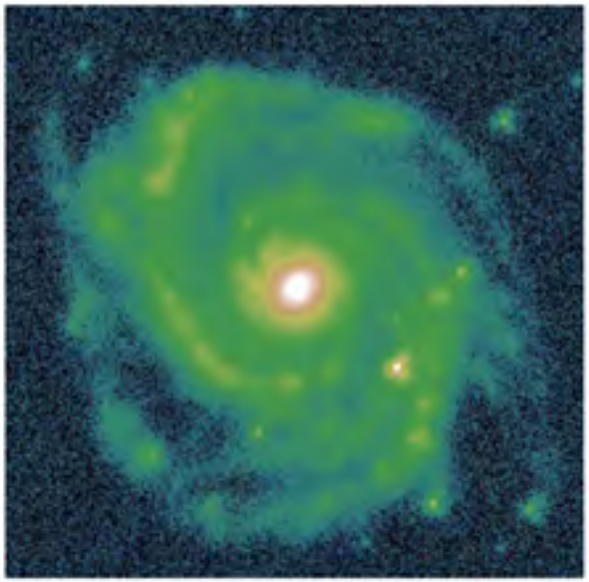

Blur is generally modeled as a linear transformation applied on the original crisp image.

Within the anisoplanatism domain, this transformation is a convolution:

$$\mathcal{M}[f](\boldsymbol{r}) \equiv \int h(\boldsymbol{r}-\boldsymbol{s}) f(\boldsymbol{s})\, \mathrm{d}\boldsymbol{s}$$

The 3 ingredients of a deblurring method

1. The degradation model 2/2: noise

Noise is considered as a stochastic perturbation of the image (it may have a deterministic origin, e.g., quantization noise).

The simplest (and most used) model is white Gaussian noise. The probability density function is then:

$$-\log p\,(\,g(\boldsymbol{r})\,|\,\mathcal{M}[f](\boldsymbol{r})\,) \propto \frac{(\,g(\boldsymbol{r}) - \mathcal{M}[f](\boldsymbol{r})\,)^2}{\sigma^2} + \text{cste}$$

Under low/moderate light flux, it is more accurate to vary the variance of noise σ^2 with the signal amplitude $\mathcal{M}[f](\boldsymbol{r})$.
At very low levels of light (photon counting), or under coherent lighting non-Gaussian pdf are more accurate (e.g., mix of Poisson and Gaussian, gamma distributions for speckle).
Noise at different pixels may show some correlations. This can be modeled through a non-diagonal covariance matrix $\boldsymbol{\Sigma} = \boldsymbol{W}^{-1}$:

$$-\log p\,(\,\boldsymbol{g}\,|\,\mathcal{M}[\boldsymbol{f}]\,) \propto (\boldsymbol{g} - \mathcal{M}[\boldsymbol{f}])^{\mathrm{T}}\boldsymbol{W}(\boldsymbol{g} - \mathcal{M}[\boldsymbol{f}]) + \text{cste}$$

The 3 ingredients of a deblurring method

2. The model for the class of images considered

It is essential to constrain the recovered image to be in a restricted class of images to prevent from overfitting the noise.

The constraints take the form of regularization terms, or prior models under a Bayesian setting.

A typical example widely used in image deblurring is total variation (or relaxed versions that prevent the staircasing effect):

$$-\log p\left(\boldsymbol{f}\right) \propto \sum_i \|(\nabla \boldsymbol{f})_i\|_2$$

The 3 ingredients of a deblurring method

3. The estimator

Given the model of the degradation and of the images under consideration, an estimator can be built.

The most widely used estimator for image deblurring is the maximum *a posteriori* estimator:

$$\hat{\boldsymbol{f}}^{(\mathrm{MAP})} = \arg\min_{\boldsymbol{f}} \quad \underbrace{-\log p\left(\boldsymbol{g} \,|\, \mathcal{M}[\boldsymbol{f}]\right)}_{\text{data fitting term}} - \mu \underbrace{\log p\left(\boldsymbol{f}\right)}_{\text{regularization}}$$

Other estimators such as the posterior mean can be computed. They generally require solving more challenging computational problems (e.g., sampling high-dimensional distributions).

Handling image borders

When performing discrete convolutions of images, we need to decide how to handle the borders.

What really matters is to reconstruct more than the observed field in order to describe correctly what is seen

Illustration in the case of a very large PSF: reconstruction in digital holography:

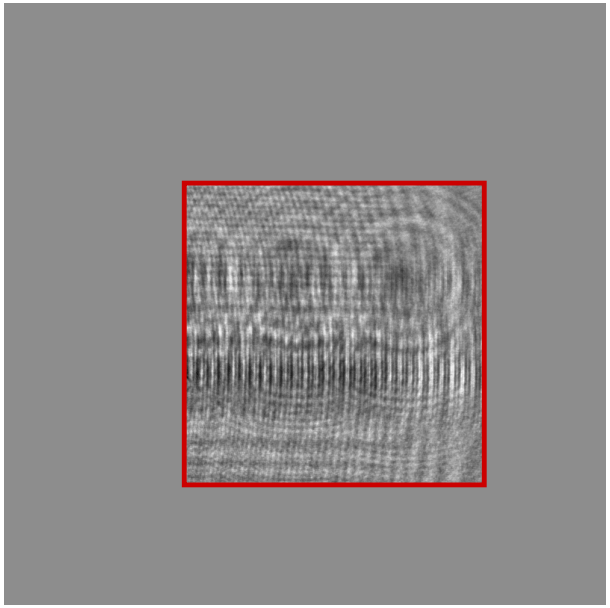

data

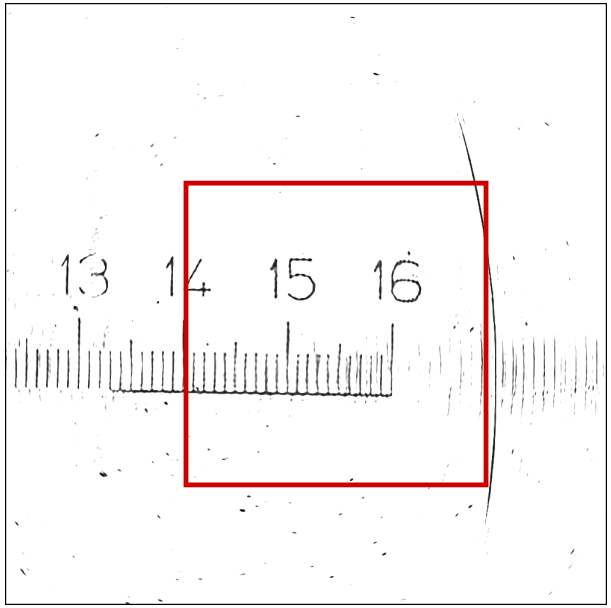

reconstruction [Denis,2009]

“Hot” topics

Some current research topics:

– learning rich statistical priors (e.g., dictionary-based: see Remi Gribonval’s talk),

– designing fast minimization methods to compute the MAP estimator (e.g., using majorant approximations: see Jérôme Idier’s talk),

– designing accurate degradation models (e.g., to account for blur variations: more on that next section),

– designing blind methods, i.e., methods that jointly estimate the original image and the PSF (more on that in last section),

– unsupervised setting of all parameters of the method.

Topics of my talk:

1. An introduction to image restoration

2. Models and inversion of shift-variant blur

3. Blind deconvolution in 3D microscopy

Blur changes in wide-field imaging

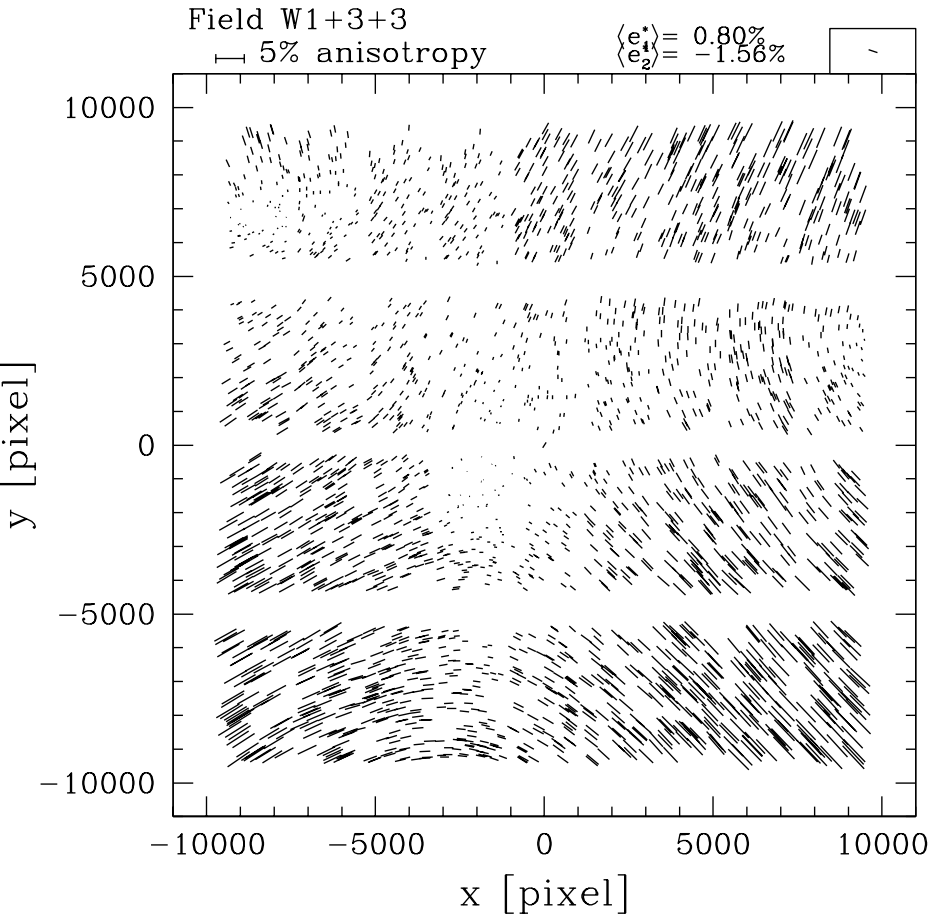

"First cosmic shear results from the Canada-France-Hawaii telescope wide synoptic legacy survey", Hoekstra *et al.*, *The Astrophysical Journal, 647 :116, 2006*

Observations of wide-fields suffer from shift-variant blurring:

– in astronomy (surveys, post adaptive optics),

– in microscopy (widening of the PSF with depth),

– in wide-angle optical systems.

→ mostly independent of the scene.

Blur variations can also occur because of scene/camera relative motion or depth-of-focus
→ depends on the 3D geometry of the scene.

Blur changes in wide-field imaging

Adaptive optics system at the VLT in Chile use laser guide stars for the correction ©ESO

Observations of wide-fields suffer from shift-variant blurring:

– in astronomy (surveys, post adaptive optics),

– in microscopy (widening of the PSF with depth),

– in wide-angle optical systems.

→ mostly independent of the scene.

Blur variations can also occur because of scene/camera relative motion or depth-of-focus
→ depends on the 3D geometry of the scene.

Blur changes in wide-field imaging

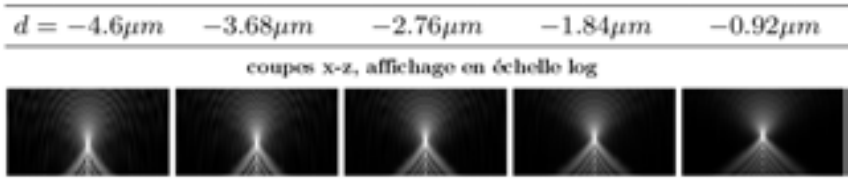

"Blind image deconvolution using machine learning for 3D microscopy", T. Kenig, Z. Kam, A. Feuer, *IEEE PAMI*, 2010.

Observations of wide-fields suffer from shift-variant blurring:

– in astronomy (surveys, post adaptive optics),

– in microscopy (widening of the PSF with depth),

– in wide-angle optical systems.

→ mostly independent of the scene.

Blur variations can also occur because of scene/camera relative motion or depth-of-focus
→ depends on the 3D geometry of the scene.

Blur changes in wide-field imaging

"Non-uniform deblurring for shaken images", O. Whyte, J. Sivic, A. Zisserman and J. Ponce, *CVPR*, 2010.

Observations of wide-fields suffer from shift-variant blurring:

– in astronomy (surveys, post adaptive optics),

– in microscopy (widening of the PSF with depth),

– in wide-angle optical systems.

→ mostly independent of the scene.

Blur variations can also occur because of scene/camera relative motion or depth-of-focus
→ depends on the 3D geometry of the scene.

Need for a fast and accurate model

If blur changes in the field of view are independent of the scene, the image formation model is still linear:

$$g(\boldsymbol{r}) = \int h(\boldsymbol{r}, \boldsymbol{s})\, f(\boldsymbol{s})\, \mathrm{d}\boldsymbol{s} \qquad \longrightarrow \qquad \boldsymbol{g} = \boldsymbol{H} \cdot \boldsymbol{f}$$

Matrix $\boldsymbol{H}$ (i.e., the direct operator) is structured in the case of shift-invariant blur (BTTB).
It can take any form in the general case of shift-variant blur. There are potentially N^2 degrees of freedom for matrix $\boldsymbol{H}$ pour N-pixels images (i.e., 10^{12} elements for mega-pixel images).

$\rightsquigarrow$ intractable for storage, application and estimation of $\boldsymbol{H}$!

We need to enforce a structure to $\boldsymbol{H}$ that achieves a trade-off between approximation quality (i.e., flexibility) and speed.

Approximating shift-variant blur: continuous point-of-view

The linear formation models write:

$$\underbrace{g(\boldsymbol{r}) = \int h(\boldsymbol{r}, \boldsymbol{s})\, f(\boldsymbol{s})\, \mathrm{d}\boldsymbol{s}}_{\text{shift-variant case}} \qquad \text{and} \qquad \underbrace{g(\boldsymbol{r}) = \int h(\boldsymbol{r} - \boldsymbol{s})\, f(\boldsymbol{s})\, \mathrm{d}\boldsymbol{s}}_{\text{shift-invariant case (convolution)}}$$

Replacing the PSF with a separable approximation:

$$h(\boldsymbol{r}, \boldsymbol{s}) \approx \sum_{i=1}^{k} m_i(\boldsymbol{r} - \boldsymbol{s})\, w_i(\boldsymbol{s})$$

leads to an efficient approximation [Gilad & Hardenberg, 2006]:

$$\underbrace{g(\boldsymbol{r}) = \int h(\boldsymbol{r}, \boldsymbol{s})\, f(\boldsymbol{s})\, \mathrm{d}\boldsymbol{s}}_{\text{shift-variant case}} \approx \int \sum_{i=1}^{k} m_i(\boldsymbol{r} - \boldsymbol{s})\, w_i(\boldsymbol{s}) f(\boldsymbol{s})\, \mathrm{d}\boldsymbol{s}$$

$$\|$$

$$\sum_{i=1}^{k} \int m_i(\boldsymbol{r} - \boldsymbol{s})\, [w_i(\boldsymbol{s}) f(\boldsymbol{s})]\, \mathrm{d}\boldsymbol{s}$$

Approximating shift-variant blur: continuous point-of-view

The linear formation models write:

$$\underbrace{g(\boldsymbol{r}) = \int h(\boldsymbol{r}, \boldsymbol{s})\, f(\boldsymbol{s})\, \mathrm{d}\boldsymbol{s}}_{\text{shift-variant case}} \qquad \text{and} \qquad \underbrace{g(\boldsymbol{r}) = \int h(\boldsymbol{r} - \boldsymbol{s})\, f(\boldsymbol{s})\, \mathrm{d}\boldsymbol{s}}_{\text{shift-invariant case (convolution)}}$$

Replacing the PSF with a separable approximation:

$$h(\boldsymbol{r}, \boldsymbol{s}) \approx \sum_{i=1}^{k} m_i(\boldsymbol{r} - \boldsymbol{s})\, w_i(\boldsymbol{s})$$

leads to an efficient approximation [Gilad & Hardenberg, 2006]:

$$\underbrace{g(\boldsymbol{r}) = \int h(\boldsymbol{r}, \boldsymbol{s})\, f(\boldsymbol{s})\, \mathrm{d}\boldsymbol{s}}_{\text{shift-variant case}} \approx \int \sum_{i=1}^{k} m_i(\boldsymbol{r} - \boldsymbol{s})\, w_i(\boldsymbol{s}) f(\boldsymbol{s})\, \mathrm{d}\boldsymbol{s}$$

$$\|$$

$$k \text{ convolutions} \quad \longleftarrow \quad \sum_{i=1}^{k} \int m_i(\boldsymbol{r} - \boldsymbol{s})\, [w_i(\boldsymbol{s}) f(\boldsymbol{s})]\, \mathrm{d}\boldsymbol{s}$$

Approximating shift-variant blur: discrete point-of-view

Let's consider the structure of the matrix $\boldsymbol{H}$:

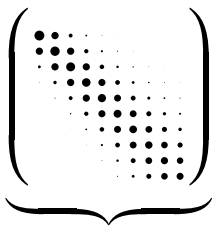

shift-variant case

and

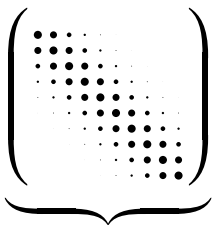

shift-invariant case (convolution)

We need to model changes of the PSF with the position:

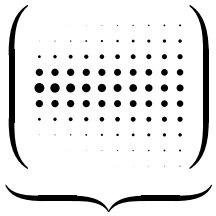

shift-variant case

and

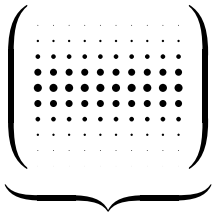

shift-invariant case (convolution)

Approximating shift-variant blur: discrete point-of-view

Possible approximations:

– piecewise-constant:

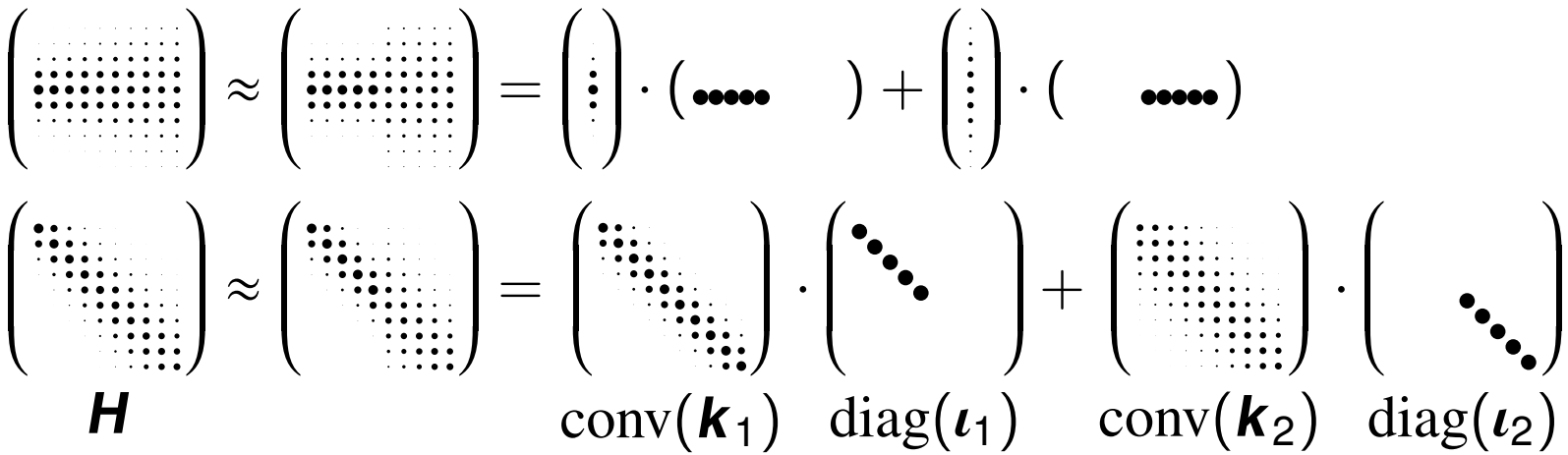

Approximating shift-variant blur: discrete point-of-view

Possible approximations:

– interpolation of PSF

[Hirsch *et al.* 2010; Denis *et al.* 2011; Ben Hadj & Blanc-Féraud 2012]

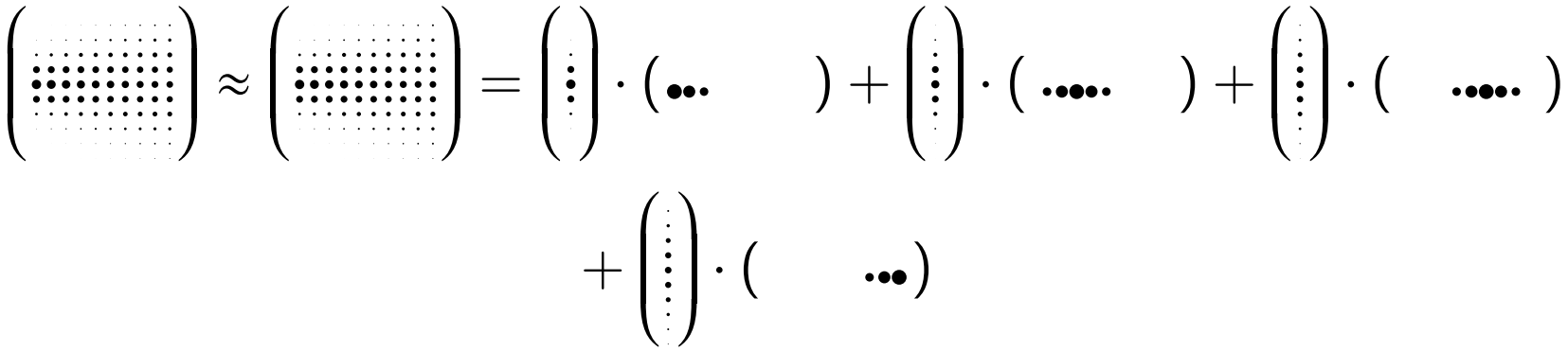

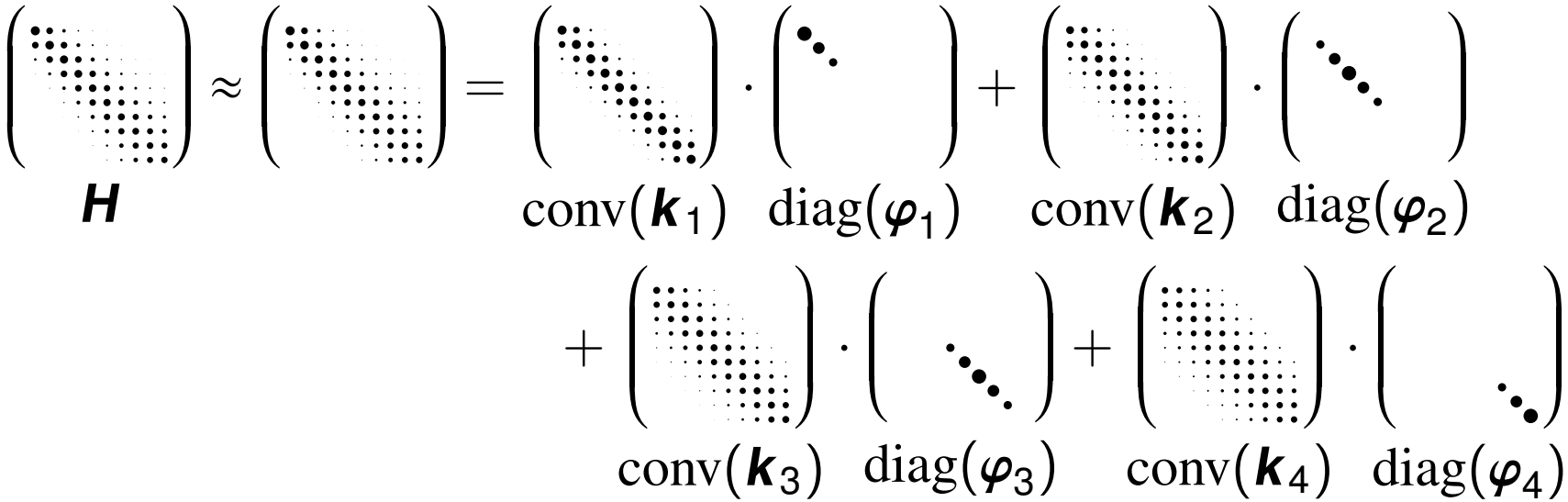

Approximating shift-variant blur: discrete point-of-view

Possible approximations:

– low-rank approximation: decomposition on PSF modes

[Flicker & Rigaut 2005; Miraut & Portilla 2012]

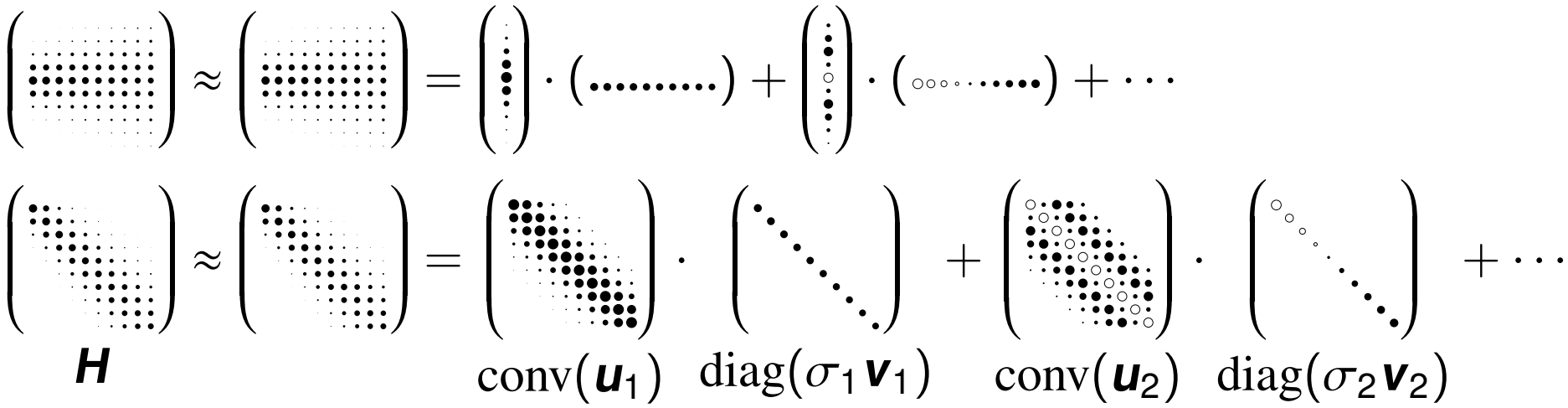

Best localized approximation

Possible approximations:

– optimal approximation with localized weights

[Denis, Thiébaut & Soulez 2011]

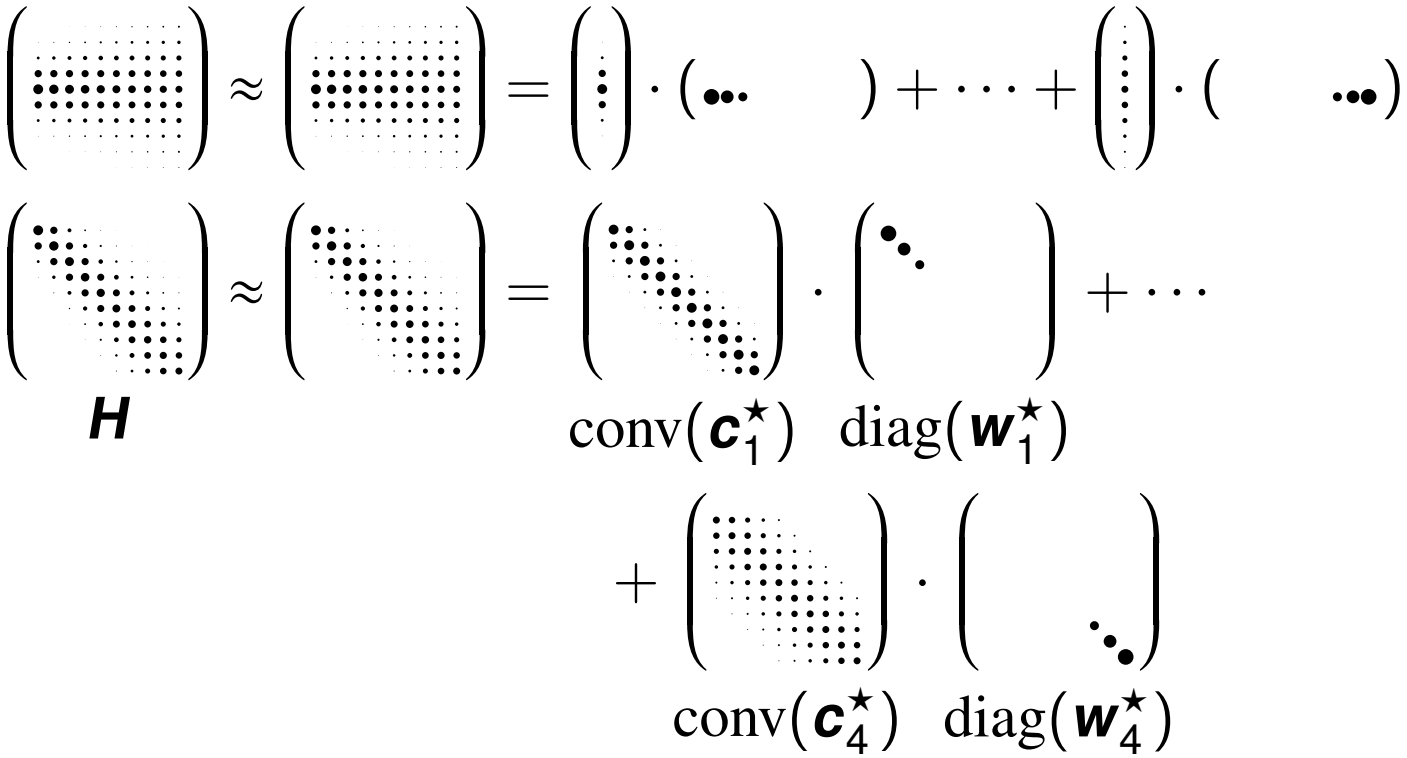

Implementation

Shift-variant blurring can be computed efficiently:

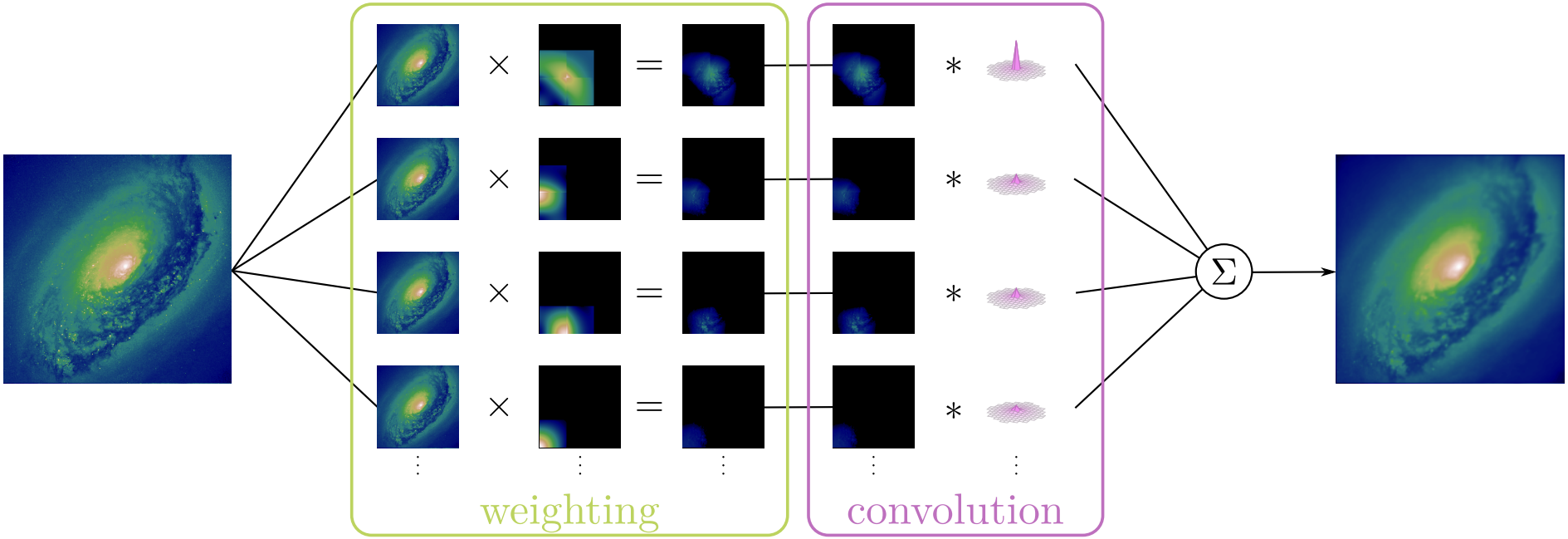

$$\boldsymbol{H}\boldsymbol{f} \approx \left[\sum_{i=1}^{k} \mathrm{conv}(m_i)\mathrm{diag}(w_i)\right]\boldsymbol{f}$$

Deblurring illustrations

Simulation of an optical system with aberrations:

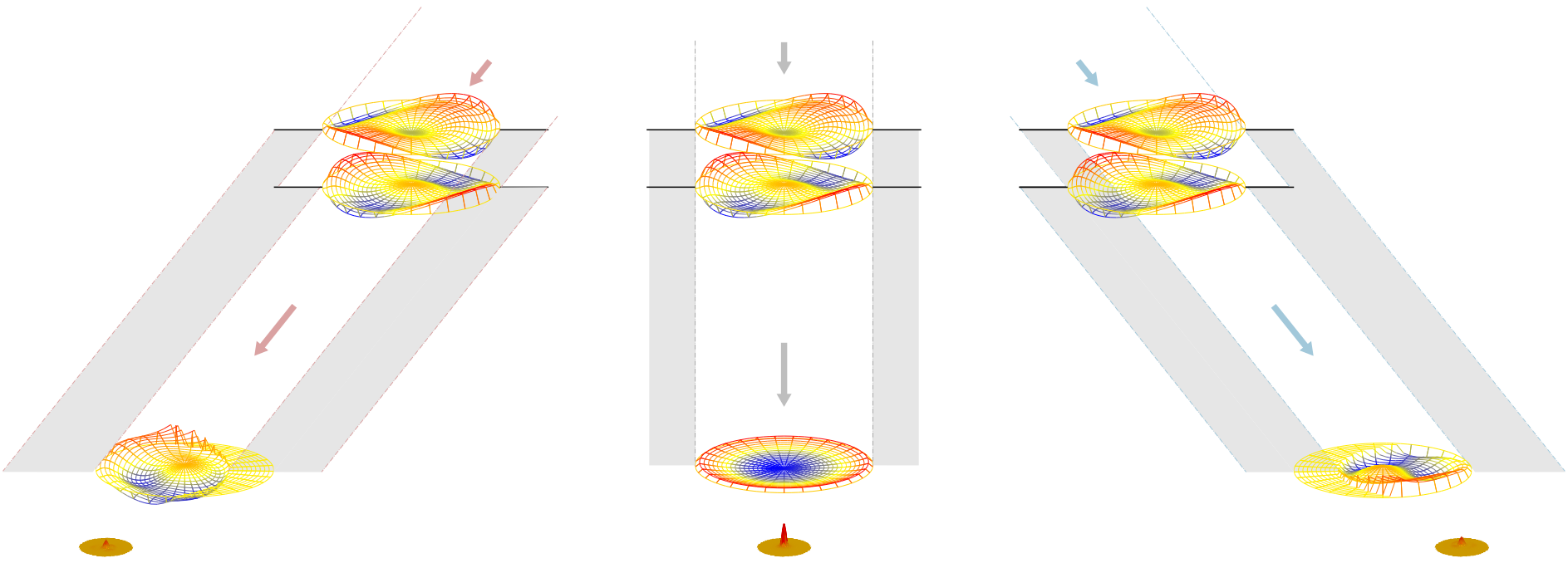

(a) (b) (c)

Deblurring illustrations

Simulation of a blurred image:

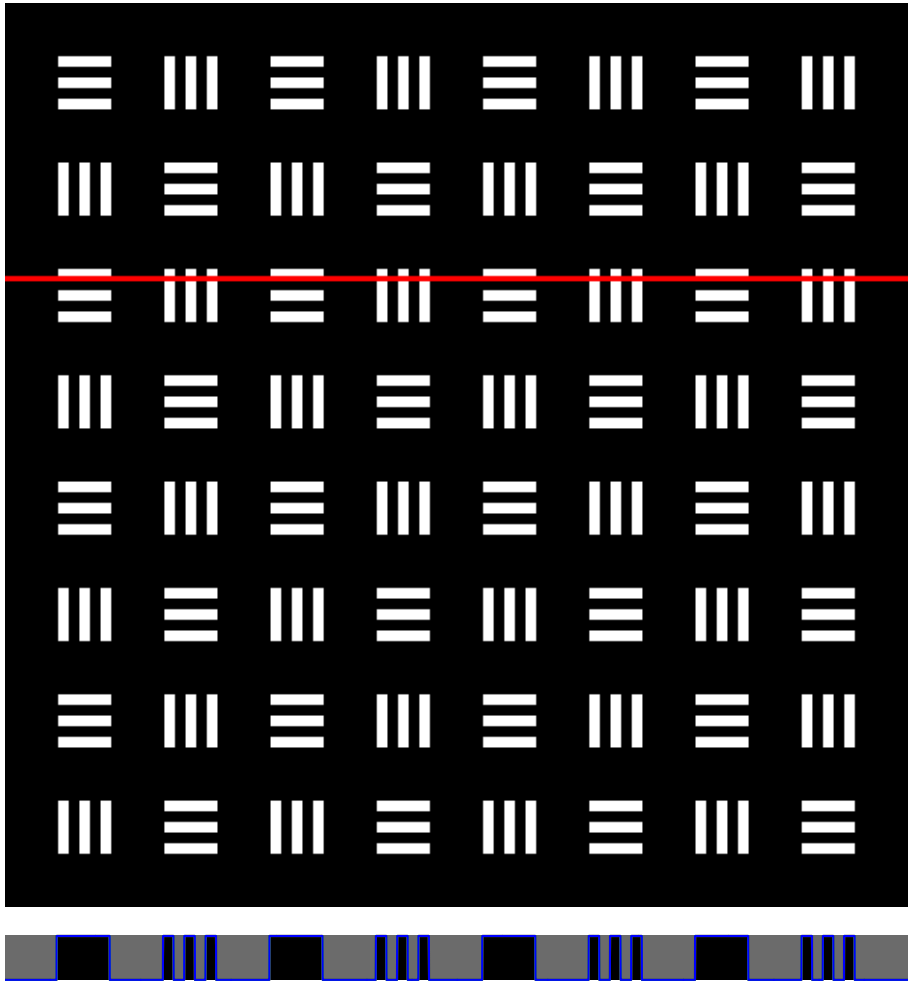

original

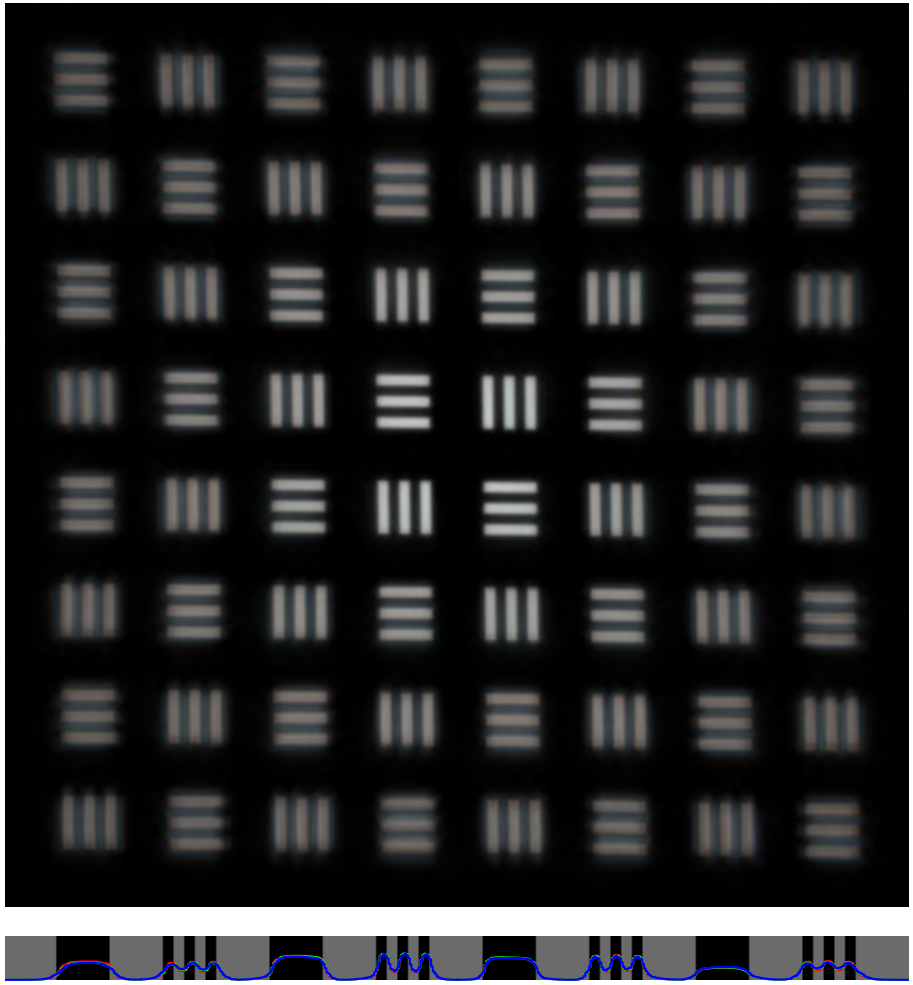

blurred

Deblurring illustrations

Deblurring results:

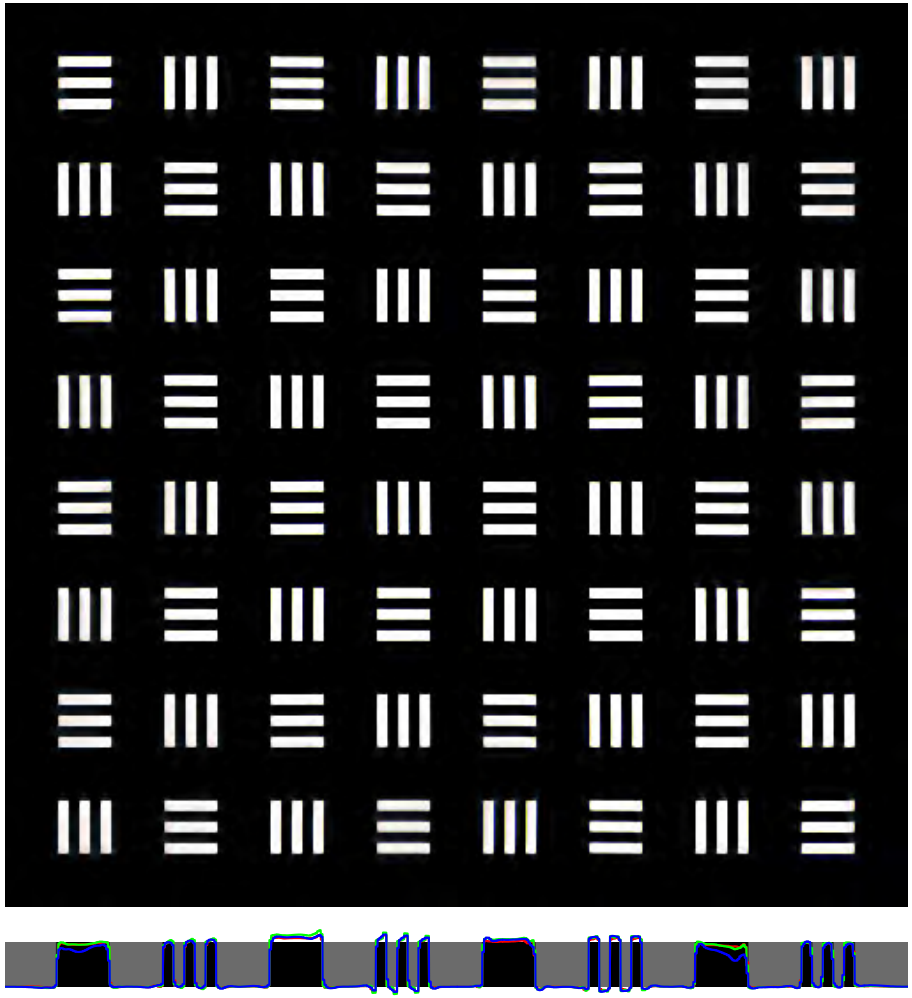

5×5 interp. PSF (PSNR=25dB)

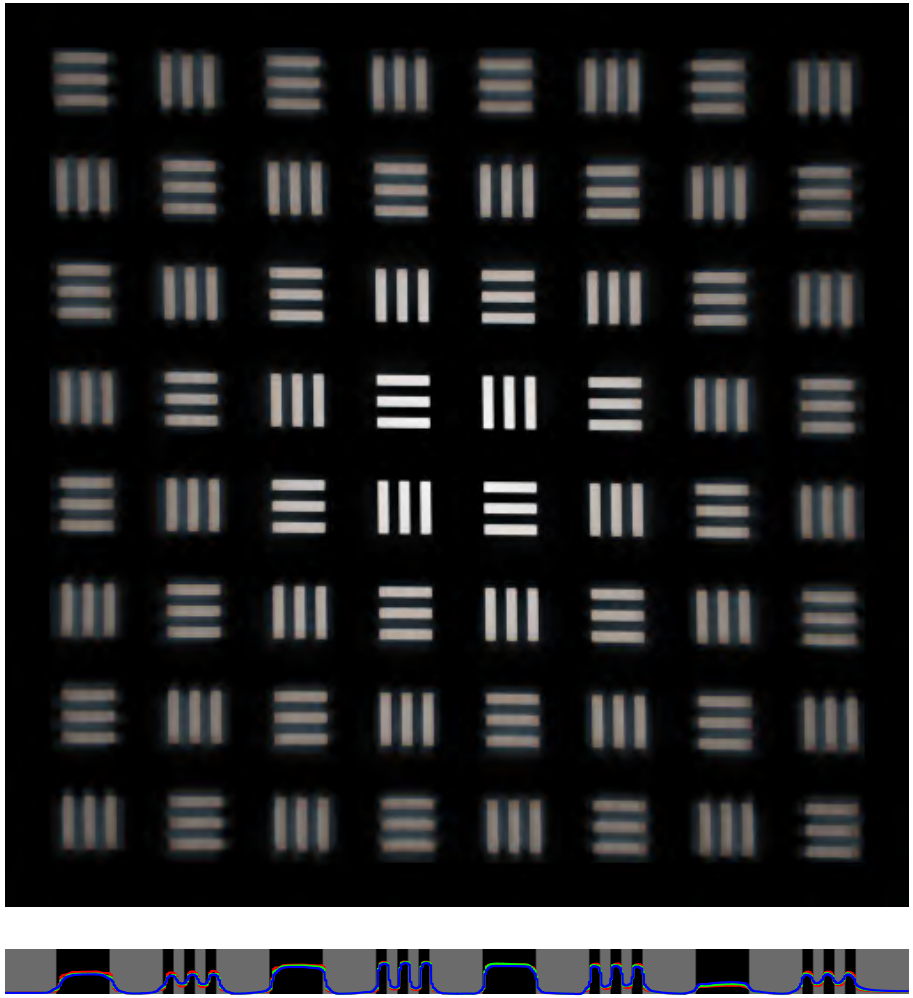

1 PSF (PSNR=12dB)

Deblurring illustrations

Deblurring results:

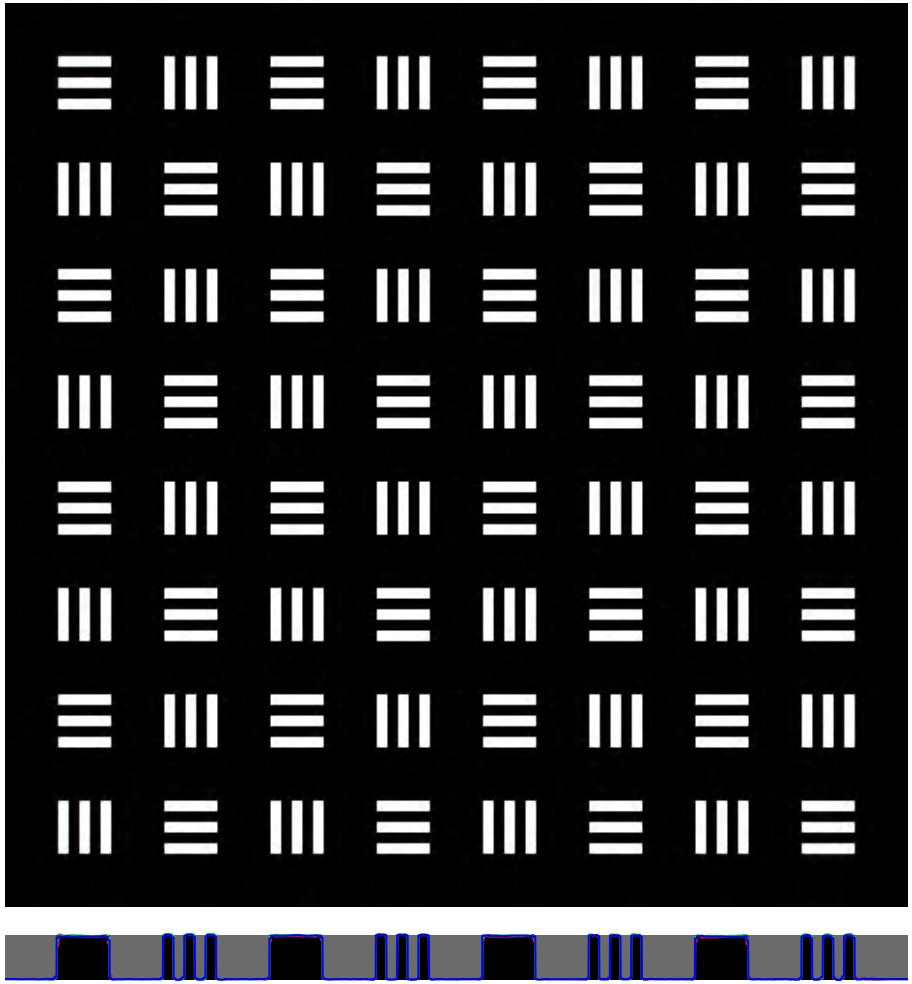

21 × 21 interp. PSF (PSNR=38dB)

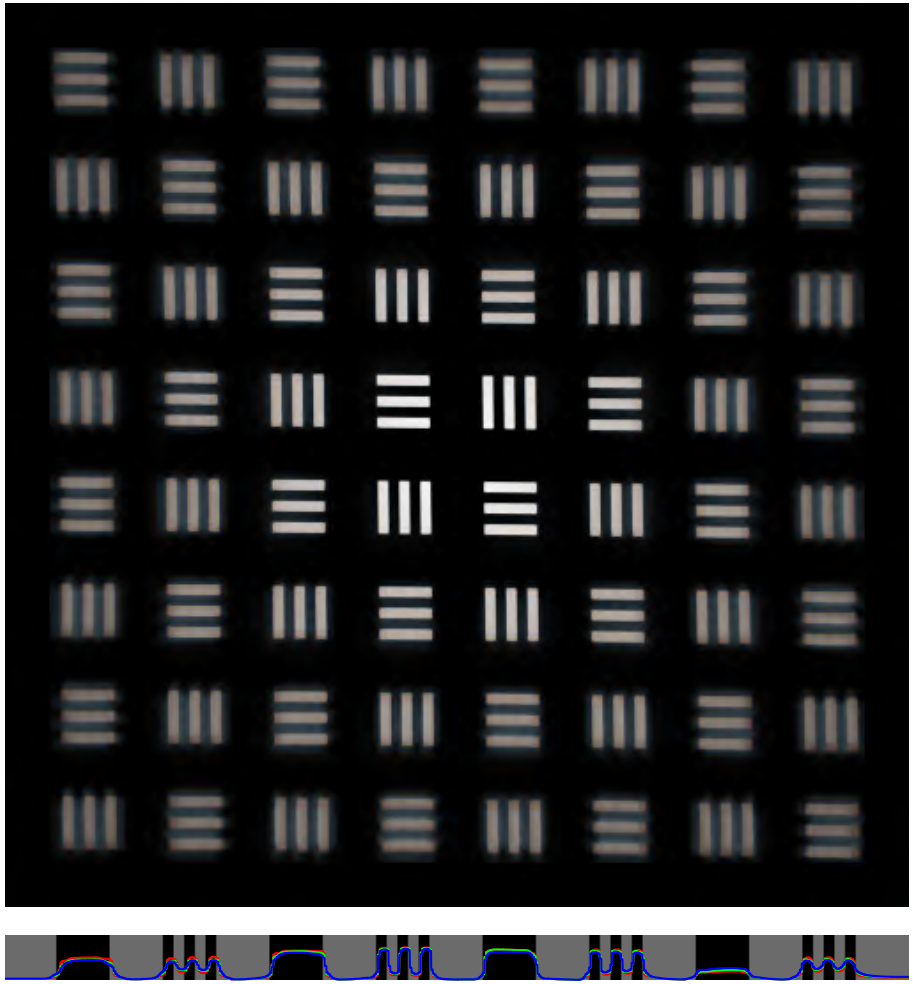

1 PSF (PSNR=12dB)

Application to spatio-spectral deblurring

Context: Hyper-spectral imaging with MUSE instrument (integral field spectrometer for deep field astronomical imaging).

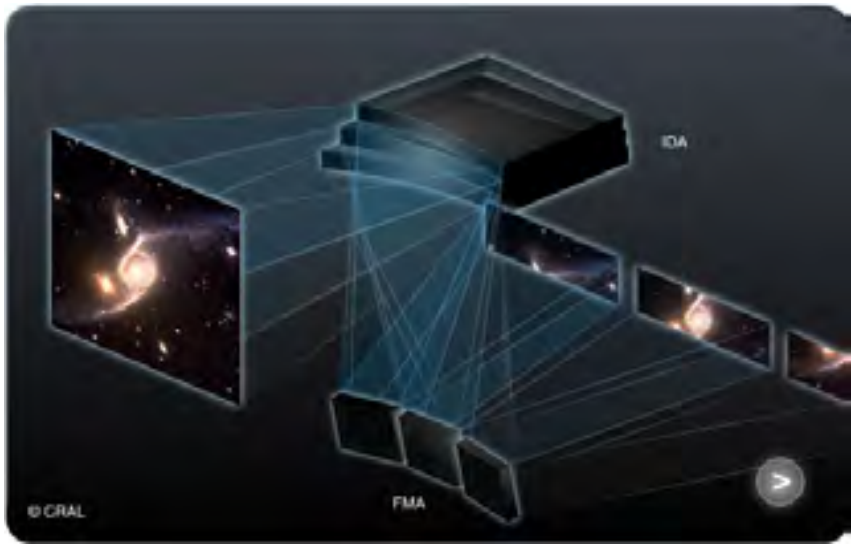

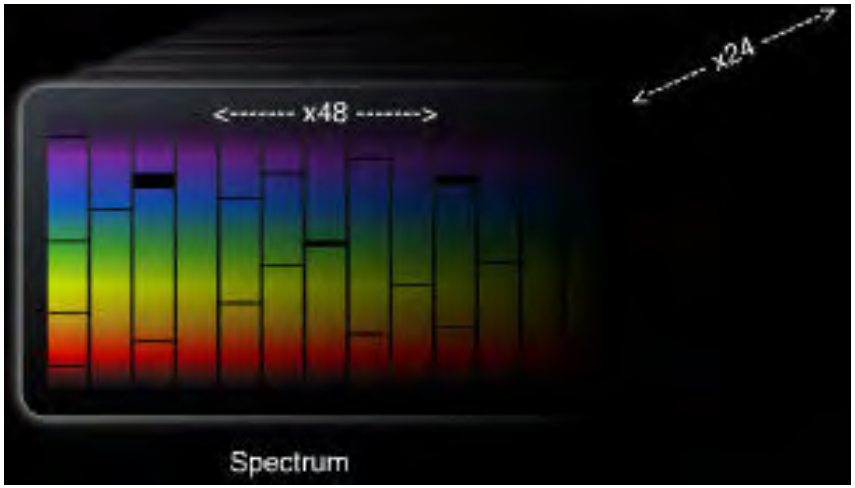

The field of view is sliced into rows. Each row of the image is then dispersed to produce a spectro-spatial 2D image.
When put together, all spectrum measured form a 3D hyperspectral cube with 300x300 pixels and 3463 bins spectrum.

Application to spatio-spectral deblurring

Problem: To improve the quality of the images, it is necessary to deblur the data.

The PSF varies smoothly with the wavelength.

It can be approximated by interpolating few PSF:

$$h_\lambda(\Delta\boldsymbol{\theta}, \Delta\lambda) \approx \sum_{i=1}^{k} h_i(\Delta\boldsymbol{\theta}, \Delta\lambda) w_i(\lambda)$$

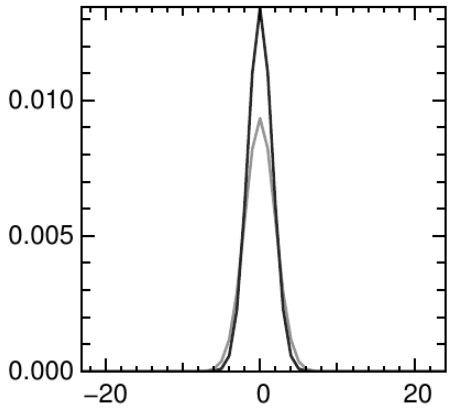

spatial profile of the PSF

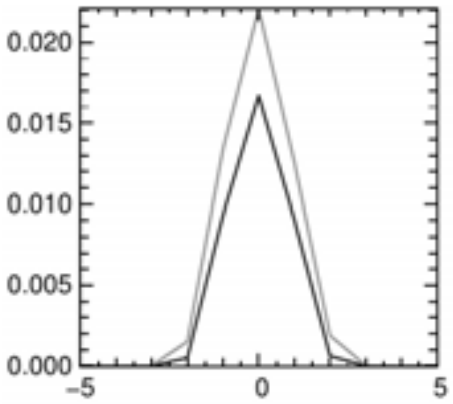

spectral profile of the PSF

Application to spatio-spectral deblurring

Result: Deblurring with spatial sparsity constraint (i.e., structured ℓ_1 norm minimization).

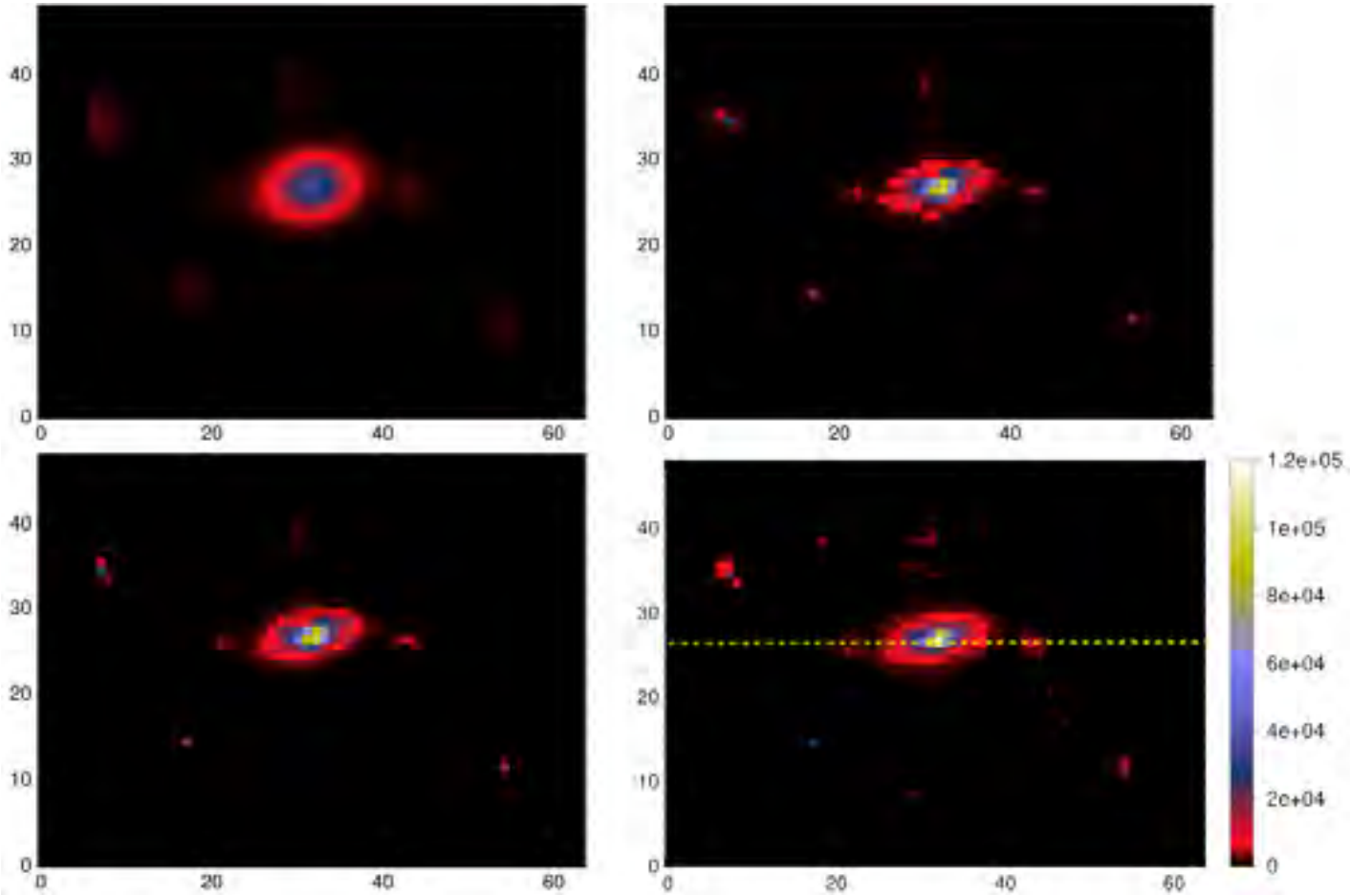

"Restoration of Hyperspectral Astronomical Data with Spectrally Varying Blur", F. Soulez *et al.*, 2013

Application to spatio-spectral deblurring

Result: Deblurring with spatial sparsity constraint (i.e., structured ℓ_1 norm minimization).

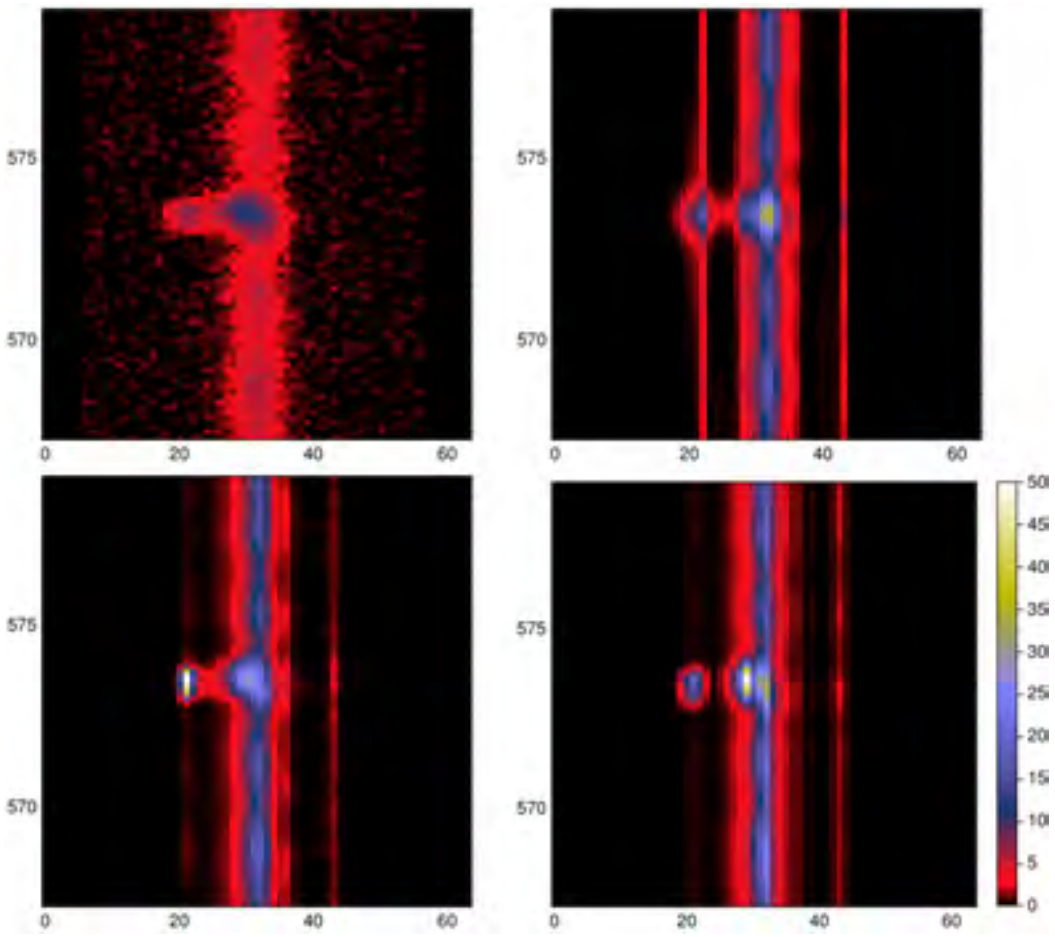

"Restoration of Hyperspectral Astronomical Data with Spectrally Varying Blur", F. Soulez *et al.*, 2013

Topics of my talk:

1. An introduction to image restoration

2. Models and inversion of shift-variant blur

3. Blind deconvolution in 3D microscopy

Wide field fluorescence microscopy

- Illumination of the whole sample,
- Observation at the emission wavelength,
- 3D image obtained by scanning the focal plane.

Very coarse depth resolution

How to improve the resolution

- Improve the PSF (confocal, multiphoton, . . .),
- Use structured illumination (SIM),
- **Deconvolution**

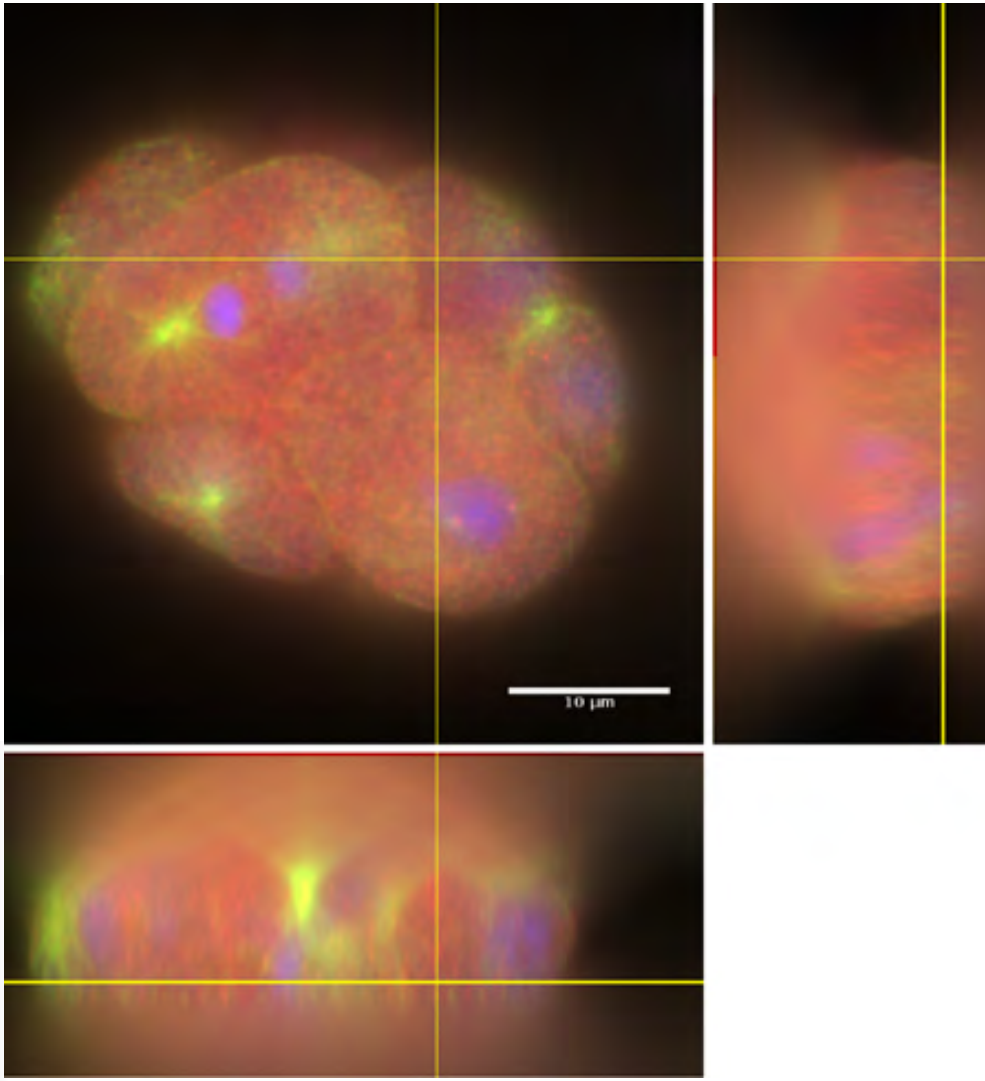

d'après [Griffa, 2010]

Wide field fluorescence microscopy

- Illumination of the whole sample,
- Observation at the emission wavelength,
- 3D image obtained by scanning the focal plane.

Very coarse depth resolution

How to improve the resolution

- Improve the PSF (confocal, multiphoton, . . .),
- Use structured illumination (SIM),
- **Deconvolution**

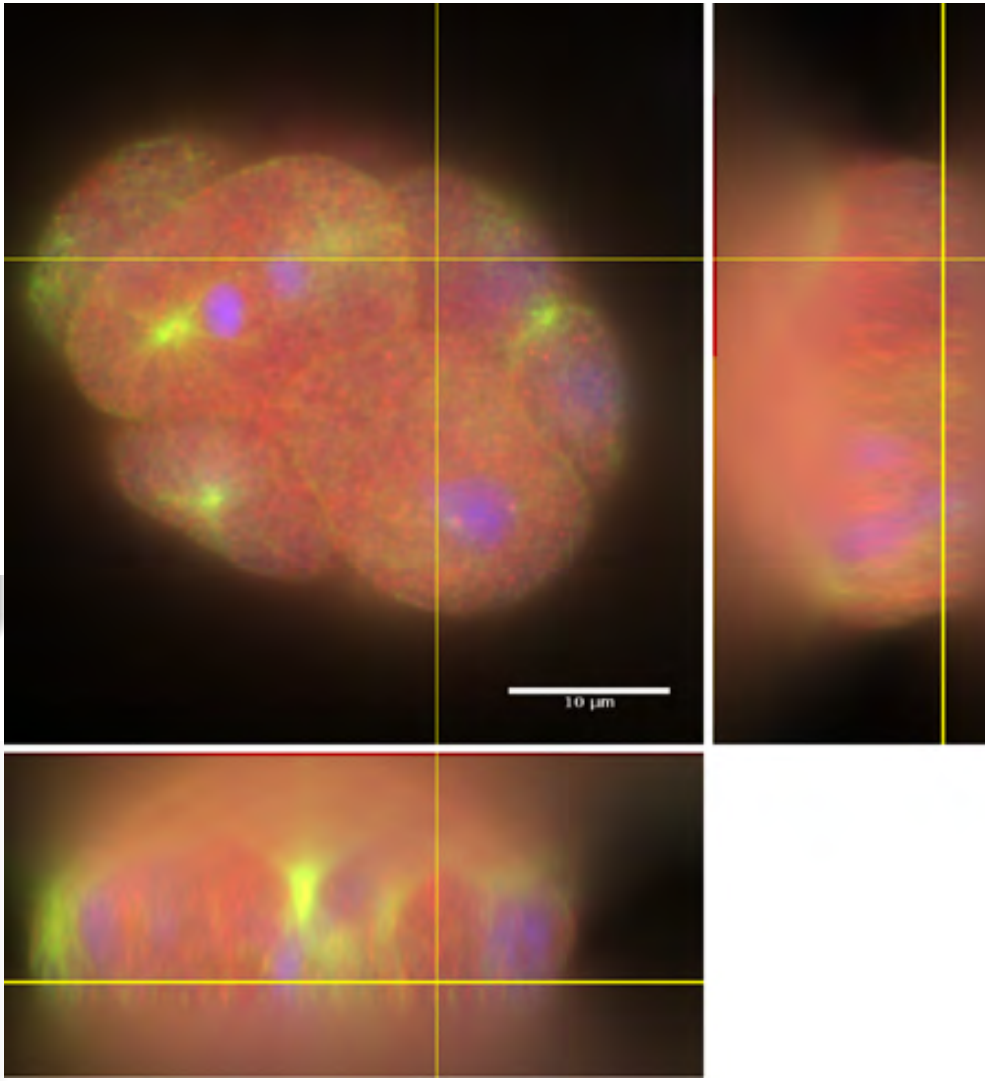

d'après [Griffa, 2010]

Wide field fluorescence microscopy

- Illumination of the whole sample,
- Observation at the emission wavelength,
- 3D image obtained by scanning the focal plane.

Very coarse depth resolution

How to improve the resolution

- Improve the PSF (confocal, multiphoton, . . .),
- Use structured illumination (SIM),
- **Deconvolution**

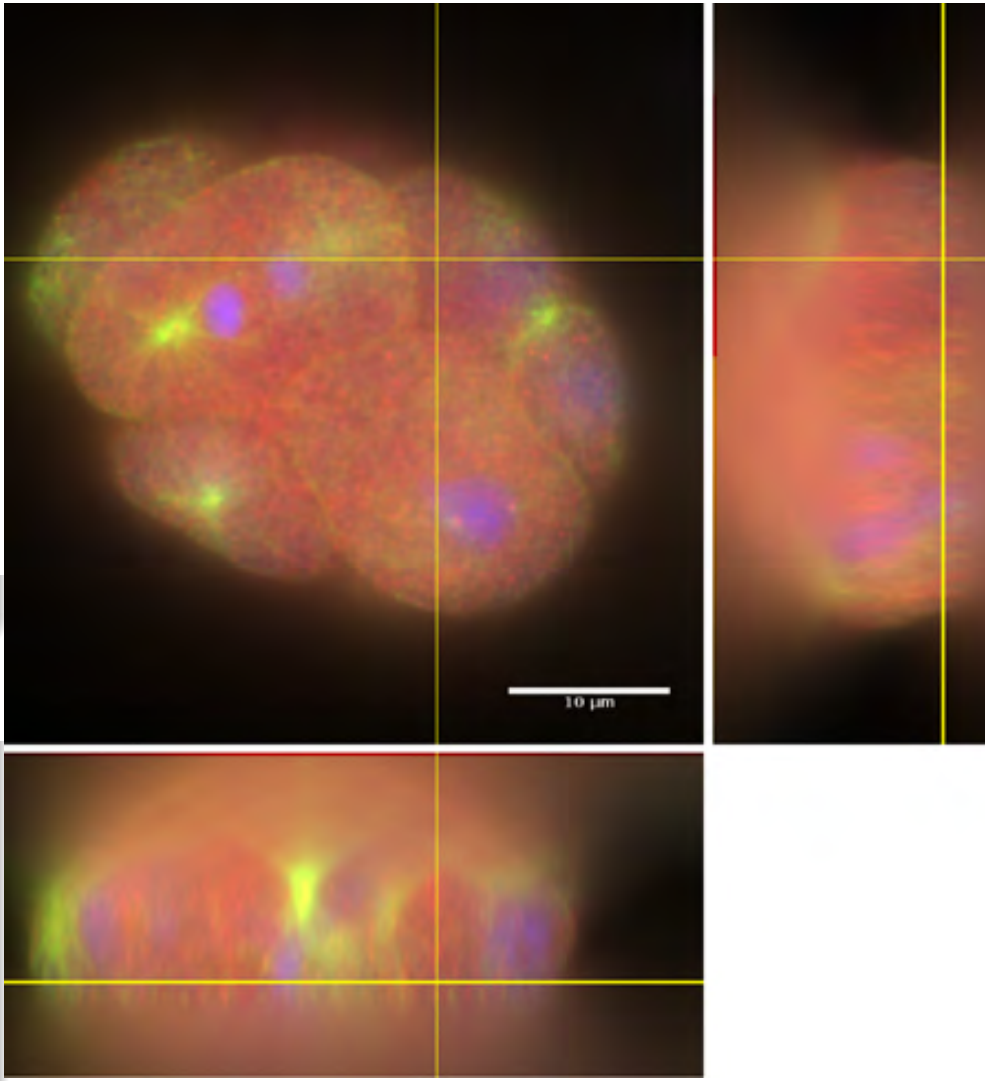

d'après [Griffa, 2010]

Blind deconvolution

Blur modeled by a convolution: Flou modélisé par la convolution :

$$\boldsymbol{g} = \boldsymbol{H}\boldsymbol{f} + \boldsymbol{n} \equiv \boldsymbol{h} * \boldsymbol{f} + \boldsymbol{n}$$

Deconvolution :
Estimate the *crisp image* $\boldsymbol{f}$ from the blurry and noisy observations $\boldsymbol{g}$, for a given *PSF* $\boldsymbol{h}$ and noise statistics.

In practice... The PSF is unknown

– use the theoretical PSF (i.e., diffraction-limited)	lacks some flexibility
– experimentally measure the PSF (beads)	hard, noisy
– direct estimation of the PSF from the data	**blind deconvolution**

Blind deconvolution

Blur modeled by a convolution: Flou modélisé par la convolution :

$$\boldsymbol{g} = \boldsymbol{H}\boldsymbol{f} + \boldsymbol{n} \equiv \boldsymbol{h} * \boldsymbol{f} + \boldsymbol{n}$$

Deconvolution :
Estimate the *crisp image* $\boldsymbol{f}$ from the blurry and noisy observations $\boldsymbol{g}$, for a given *PSF* $\boldsymbol{h}$ and noise statistics.

In practice... The PSF is unknown

– use the theoretical PSF (i.e., diffraction-limited)	lacks some flexibility
– experimentally measure the PSF (beads)	hard, noisy
– direct estimation of the PSF from the data	**blind deconvolution**

Blind deconvolution

Blur modeled by a convolution: Flou modélisé par la convolution :

$$\boldsymbol{g} = \boldsymbol{H}\boldsymbol{f} + \boldsymbol{n} \equiv \boldsymbol{h} * \boldsymbol{f} + \boldsymbol{n}$$

Deconvolution :
Estimate the *crisp image* $\boldsymbol{f}$ from the blurry and noisy observations $\boldsymbol{g}$, for a given *PSF* $\boldsymbol{h}$ and noise statistics.

In practice... The PSF is unknown

- use the theoretical PSF (i.e., diffraction-limited) — lacks some flexibility
- experimentally measure the PSF (beads) — hard, noisy
- direct estimation of the PSF from the data — **blind deconvolution**

Blind deconvolution

Blur modeled by a convolution: Flou modélisé par la convolution :

$$\boldsymbol{g} = \boldsymbol{H}\boldsymbol{f} + \boldsymbol{n} \equiv \boldsymbol{h} * \boldsymbol{f} + \boldsymbol{n}$$

Deconvolution :
Estimate the *crisp image* $\boldsymbol{f}$ from the blurry and noisy observations $\boldsymbol{g}$, for a given *PSF* $\boldsymbol{h}$ and noise statistics.

In practice... The PSF is unknown

- use the theoretical PSF (i.e., diffraction-limited) — lacks some flexibility
- experimentally measure the PSF (beads) — hard, noisy
- direct estimation of the PSF from the data — **blind deconvolution**

Blind deconvolution

Blur modeled by a convolution: Flou modélisé par la convolution :

$$\boldsymbol{g} = \boldsymbol{H}\boldsymbol{f} + \boldsymbol{n} \equiv \boldsymbol{h} * \boldsymbol{f} + \boldsymbol{n}$$

Deconvolution :
Estimate the *crisp image* $\boldsymbol{f}$ from the blurry and noisy observations $\boldsymbol{g}$, for a given *PSF* $\boldsymbol{h}$ and noise statistics.

In practice... The PSF is unknown

– use the theoretical PSF (i.e., diffraction-limited)	lacks some flexibility
– experimentally measure the PSF (beads)	hard, noisy
– direct estimation of the PSF from the data	**blind deconvolution**

Blind deconvolution

Blur modeled by a convolution: Flou modélisé par la convolution :

$$\boldsymbol{g} = \boldsymbol{H}\boldsymbol{f} + \boldsymbol{n} \equiv \boldsymbol{h} * \boldsymbol{f} + \boldsymbol{n}$$

Deconvolution :
Estimate the *crisp image* $\boldsymbol{f}$ from the blurry and noisy observations $\boldsymbol{g}$, for a given *PSF* $\boldsymbol{h}$ and noise statistics.

In practice... The PSF is unknown

– use the theoretical PSF (i.e., diffraction-limited)	lacks some flexibility
– experimentally measure the PSF (beads)	hard, noisy
– direct estimation of the PSF from the data	**blind deconvolution**

Blind deconvolution

Blur modeled by a convolution: Flou modélisé par la convolution :

$$\boldsymbol{g} = \boldsymbol{H}\boldsymbol{f} + \boldsymbol{n} \equiv \boldsymbol{h} * \boldsymbol{f} + \boldsymbol{n}$$

Deconvolution :
Estimate the *crisp image* $\boldsymbol{f}$ from the blurry and noisy observations $\boldsymbol{g}$, for a given *PSF* $\boldsymbol{h}$ and noise statistics.

In practice... The PSF is unknown

- use the theoretical PSF (i.e., diffraction-limited) — lacks some flexibility
- experimentally measure the PSF (beads) — hard, noisy
- direct estimation of the PSF from the data — **blind deconvolution**

Blind deconvolution

Blur modeled by a convolution: Flou modélisé par la convolution :

$$\boldsymbol{g} = \boldsymbol{H}\boldsymbol{f} + \boldsymbol{n} \equiv \boldsymbol{h} * \boldsymbol{f} + \boldsymbol{n}$$

Deconvolution :
Estimate the *crisp image* $\boldsymbol{f}$ from the blurry and noisy observations $\boldsymbol{g}$, for a given *PSF* $\boldsymbol{h}$ and noise statistics.

In practice... The PSF is unknown

– use the theoretical PSF (i.e., diffraction-limited)	lacks some flexibility
– experimentally measure the PSF (beads)	hard, noisy
– direct estimation of the PSF from the data	**blind deconvolution**

Degradation model

- Gaussian noise :

$$\text{data fitting term:} \quad (\boldsymbol{g} - \boldsymbol{H} \cdot \boldsymbol{f})^{\mathrm{T}} \cdot \boldsymbol{\Sigma}^{-1} \cdot (\boldsymbol{g} - \boldsymbol{H} \cdot \boldsymbol{f})$$

- Unstationary white noise :

$$\text{data fitting term:} \quad \sum_{\text{pixels } j} \frac{1}{\sigma_j^2} \left[(\boldsymbol{H} \cdot \boldsymbol{f})_j - g_j \right]^2$$

Missing pixels $\longrightarrow \sigma_j^2 = \infty$.

- Photon noise $\approx$ unstationary Gaussian noise

$$\sigma_j = \gamma (\boldsymbol{H} \cdot \boldsymbol{f})_j + \sigma_{\mathrm{a}}^2 \approx \gamma \max(g_j, 0) + \sigma_{\mathrm{a}}^2$$

γ: quantization gain
σ_{a}^2: additive noise sources (*e.g.* reading noise...).

Degradation model

- Gaussian noise :

$$\text{data fitting term:} \quad (\boldsymbol{g} - \boldsymbol{H} \cdot \boldsymbol{f})^{\mathrm{T}} \cdot \boldsymbol{\Sigma}^{-1} \cdot (\boldsymbol{g} - \boldsymbol{H} \cdot \boldsymbol{f})$$

- Unstationary white noise :

$$\text{data fitting term:} \quad \sum_{\text{pixels } j} \frac{1}{\sigma_j^2} \left[(\boldsymbol{H} \cdot \boldsymbol{f})_j - g_j \right]^2$$

Missing pixels $\longrightarrow \sigma_j^2 = \infty$.

- Photon noise $\approx$ unstationary Gaussian noise

$$\sigma_j = \gamma (\boldsymbol{H} \cdot \boldsymbol{f})_j + \sigma_{\mathrm{a}}^2 \approx \gamma \max(g_j, 0) + \sigma_{\mathrm{a}}^2$$

γ: quantization gain
σ_{a}^2: additive noise sources (*e.g.* reading noise. . .).

Degradation model

- Gaussian noise :

$$\text{data fitting term:} \quad (\boldsymbol{g} - \boldsymbol{H} \cdot \boldsymbol{f})^{\mathrm{T}} \cdot \boldsymbol{\Sigma}^{-1} \cdot (\boldsymbol{g} - \boldsymbol{H} \cdot \boldsymbol{f})$$

- Unstationary white noise :

$$\text{data fitting term:} \quad \sum_{\text{pixels } j} \frac{1}{\sigma_j^2} \left[(\boldsymbol{H} \cdot \boldsymbol{f})_j - g_j \right]^2$$

Missing pixels $\longrightarrow \sigma_j^2 = \infty$.

- Photon noise $\approx$ unstationary Gaussian noise

$$\sigma_j = \gamma (\boldsymbol{H} \cdot \boldsymbol{f})_j + \sigma_{\mathrm{a}}^2 \approx \gamma \max(g_j, 0) + \sigma_{\mathrm{a}}^2$$

γ: quantization gain
σ_{a}^2: additive noise sources (*e.g.* reading noise...).

Degradation model: PSF parameterization

The PSF $\boldsymbol{h}$ is defined by the pupil function [Markham,1999; Hanser,2004]

$$h(\boldsymbol{r}_j, z) = \left| \sum_k F_{j,k}\, a_k(z) \right|^2 ,$$

with $\boldsymbol{r}_j$ the location of pixel j, $\boldsymbol{F}$ the discrete Fourier transform, $a_k(z)$ the pupil function at frequency k and at depth z.

$$a_k(z) = \rho_k \, \exp(\mathrm{i}\, 2\pi\, (\phi_k + z\, \psi_k)) \ ,$$

$$\rho_k = \sum_n \beta_n Z_k^n \ ,$$

$$\phi_k = \sum_n \alpha_n Z_k^n \ ,$$

$$\psi_k = \sqrt{k_\mathrm{i}^2 - (\kappa_x - \delta_x)^2 - (\kappa_y - \delta_y)^2}$$

Z_k^n: n-th Zernike polynomial, $k_0 = (n_\mathrm{i}/\lambda)$ with n_i: optical index and (δ_x, δ_y): the location of the optical axis.

PSF parameterized by $\{k_0, \alpha, \beta, \delta_x, \delta_y\}$

Degradation model: PSF parameterization

The PSF $\boldsymbol{h}$ is defined by the pupil function [Markham,1999; Hanser,2004]

$$h(\boldsymbol{r}_j, z) = \left| \sum_k F_{j,k}\, a_k(z) \right|^2 ,$$

with $\boldsymbol{r}_j$ the location of pixel j, $\boldsymbol{F}$ the discrete Fourier transform, $a_k(z)$ the pupil function at frequency k and at depth z.

$$a_k(z) = \rho_k \, \exp(\mathrm{i}\, 2\pi\, (\phi_k + z\, \psi_k)) ,$$

$$\rho_k = \sum_n \beta_n Z_k^n ,$$

$$\phi_k = \sum_n \alpha_n Z_k^n ,$$

$$\psi_k = \sqrt{k_\mathrm{i}^2 - (\kappa_x - \delta_x)^2 - (\kappa_y - \delta_y)^2}$$

Z_k^n: n-th Zernike polynomial, $k_0 = (n_\mathrm{i}/\lambda)$ with n_i: optical index and (δ_x, δ_y): the location of the optical axis.

PSF parameterized by $\{k_0, \alpha, \beta, \delta_x, \delta_y\}$

Degradation model: PSF parameterization

The PSF $\boldsymbol{h}$ is defined by the pupil function [Markham,1999; Hanser,2004]

$$h(\boldsymbol{r}_j, z) = \left| \sum_k F_{j,k}\, a_k(z) \right|^2 ,$$

with $\boldsymbol{r}_j$ the location of pixel j, $\boldsymbol{F}$ the discrete Fourier transform, $a_k(z)$ the pupil function at frequency k and at depth z.

$$a_k(z) = \rho_k \, \exp(\mathrm{i}\, 2\pi\, (\phi_k + z\, \psi_k)) ,$$

$$\rho_k = \sum_n \beta_n Z_k^n ,$$

$$\phi_k = \sum_n \alpha_n Z_k^n ,$$

$$\psi_k = \sqrt{k_\mathrm{i}^2 - (\kappa_x - \delta_x)^2 - (\kappa_y - \delta_y)^2}$$

Z_k^n: n-th Zernike polynomial, $k_0 = (n_\mathrm{i}/\lambda)$ with n_i: optical index and (δ_x, δ_y): the location of the optical axis.

PSF parameterized by $\{k_0, \alpha, \beta, \delta_x, \delta_y\}$

Degradation model: PSF parameterization

The PSF $\boldsymbol{h}$ is defined by the pupil function [Markham,1999; Hanser,2004]

$$h(\boldsymbol{r}_j, z) = \left| \sum_k F_{j,k}\, a_k(z) \right|^2 ,$$

with $\boldsymbol{r}_j$ the location of pixel j, $\boldsymbol{F}$ the discrete Fourier transform, $a_k(z)$ the pupil function at frequency k and at depth z.

$$a_k(z) = \rho_k \, \exp(\mathrm{i}\, 2\pi\, (\phi_k + z\, \psi_k)) \ ,$$

$$\rho_k = \sum_n \beta_n Z_k^n \, ,$$

$$\phi_k = \sum_n \alpha_n Z_k^n \, ,$$

$$\psi_k = \sqrt{k_\mathrm{i}^2 - (\kappa_x - \delta_x)^2 - (\kappa_y - \delta_y)^2}$$

Z_k^n: n-th Zernike polynomial, $k_0 = (n_\mathrm{i}/\lambda)$ with n_i: optical index and (δ_x, δ_y): the location of the optical axis.

PSF parameterized by $\{k_0, \alpha, \beta, \delta_x, \delta_y\}$

Degradation model: PSF parameterization

The PSF $\boldsymbol{h}$ is defined by the pupil function [Markham,1999; Hanser,2004]

$$h(\boldsymbol{r}_j, z) = \left| \sum_k F_{j,k}\, a_k(z) \right|^2 ,$$

with $\boldsymbol{r}_j$ the location of pixel j, $\boldsymbol{F}$ the discrete Fourier transform, $a_k(z)$ the pupil function at frequency k and at depth z.

$$\begin{aligned} a_k(z) &= \rho_k \, \exp(\mathrm{i}\, 2\pi\, (\phi_k + z\, \psi_k)) \ , \\ \rho_k &= \sum_n \beta_n Z_k^n \, , \\ \phi_k &= \sum_n \alpha_n Z_k^n \, , \\ \psi_k &= \sqrt{k_\mathrm{i}^2 - (\kappa_x - \delta_x)^2 - (\kappa_y - \delta_y)^2} \end{aligned}$$

Z_k^n: n-th Zernike polynomial, $k_0 = (n_\mathrm{i}/\lambda)$ with n_i: optical index and (δ_x, δ_y): the location of the optical axis.

PSF parameterized by $\{k_0, \alpha, \beta, \delta_x, \delta_y\}$

Degradation model: PSF parameterization

The PSF $\boldsymbol{h}$ is defined by the pupil function [Markham,1999; Hanser,2004]

$$h(\boldsymbol{r}_j, z) = \left| \sum_k F_{j,k}\, a_k(z) \right|^2 ,$$

with $\boldsymbol{r}_j$ the location of pixel j, $\boldsymbol{F}$ the discrete Fourier transform, $a_k(z)$ the pupil function at frequency k and at depth z.

$$\begin{aligned} a_k(z) &= \rho_k \, \exp(\mathrm{i}\, 2\pi\, (\phi_k + z\, \psi_k)) \ , \\ \rho_k &= \sum_n \beta_n Z_k^n \, , \\ \phi_k &= \sum_n \alpha_n Z_k^n \, , \\ \psi_k &= \sqrt{k_\mathrm{i}^2 - (\kappa_x - \delta_x)^2 - (\kappa_y - \delta_y)^2} \end{aligned}$$

Z_k^n: n-th Zernike polynomial, $k_0 = (n_\mathrm{i}/\lambda)$ with n_i: optical index and (δ_x, δ_y): the location of the optical axis.

PSF parameterized by $\{k_0, \alpha, \boldsymbol{\beta}, \delta_x, \delta_y\}$

Interest of this parameterization

- model derived from optics (realistic PSF, positive . . .),
- requires only the knowledge of the wavelength λ and the numerical aperture NA,
- few parameters (a few tenths),
- no other prior: no regularization, no hyperparameter to tune,
- possible simplifications (*e.g.* use of only radial modes to obtain a symmetrical PSF).

Suppression of degeneracies

Degeneracies of blind deconvolution:

– permutation	$\boldsymbol{x} * \boldsymbol{h} = \boldsymbol{h} * \boldsymbol{x}$	object $\neq$ diffraction pattern
– scaling	$(\alpha\, \boldsymbol{x}) * \boldsymbol{h} = \boldsymbol{x} * \left(\frac{1}{\alpha}\boldsymbol{h}\right)$	normalized PSF: $\sum_n \beta_n^2 = 1$
– shift	$\boldsymbol{x} * \boldsymbol{h} = (\boldsymbol{\delta}_{-s} * \boldsymbol{x}) * (\boldsymbol{\delta}_s * \boldsymbol{h})$	centered PSF $\alpha_1 = \alpha_2 = 0$ (tip-tilt)
– identity	$\boldsymbol{\delta} * \boldsymbol{y} = \boldsymbol{y}$	limited bandwidth: $\boldsymbol{h} \neq \boldsymbol{\delta}$
– reducibility	$(\boldsymbol{g} * \boldsymbol{x}) * \boldsymbol{h} = \boldsymbol{x} * (\boldsymbol{g} * \boldsymbol{h})$	empirical evidence
– inversion	$\boldsymbol{x} * \boldsymbol{h} = (\boldsymbol{s} * \boldsymbol{x}) * \left(\boldsymbol{s}^{-1} * \boldsymbol{h}\right)$	empirical evidence

The proposed parameterization solves classical blind deconvolution degeneracies.

Suppression of degeneracies

Degeneracies of blind deconvolution:

– permutation	$\boldsymbol{x} * \boldsymbol{h} = \boldsymbol{h} * \boldsymbol{x}$	object $\neq$ diffraction pattern
– scaling	$(\alpha\, \boldsymbol{x}) * \boldsymbol{h} = \boldsymbol{x} * \left(\frac{1}{\alpha}\boldsymbol{h}\right)$	normalized PSF: $\sum_n \beta_n^2 = 1$
– shift	$\boldsymbol{x} * \boldsymbol{h} = (\boldsymbol{\delta}_{-s} * \boldsymbol{x}) * (\boldsymbol{\delta}_s * \boldsymbol{h})$	centered PSF $\alpha_1 = \alpha_2 = 0$ (tip-tilt)
– identity	$\boldsymbol{\delta} * \boldsymbol{y} = \boldsymbol{y}$	limited bandwidth: $\boldsymbol{h} \neq \boldsymbol{\delta}$
– reducibility	$(\boldsymbol{g} * \boldsymbol{x}) * \boldsymbol{h} = \boldsymbol{x} * (\boldsymbol{g} * \boldsymbol{h})$	empirical evidence
– inversion	$\boldsymbol{x} * \boldsymbol{h} = (\boldsymbol{s} * \boldsymbol{x}) * \left(\boldsymbol{s}^{-1} * \boldsymbol{h}\right)$	empirical evidence

The proposed parameterization solves classical blind deconvolution degeneracies.

Suppression of degeneracies

Degeneracies of blind deconvolution:

– permutation	$\boldsymbol{x} * \boldsymbol{h} = \boldsymbol{h} * \boldsymbol{x}$	object $\neq$ diffraction pattern
– scaling	$(\alpha\, \boldsymbol{x}) * \boldsymbol{h} = \boldsymbol{x} * \left(\frac{1}{\alpha}\boldsymbol{h}\right)$	normalized PSF: $\sum_n \beta_n^2 = 1$
– shift	$\boldsymbol{x} * \boldsymbol{h} = (\boldsymbol{\delta}_{-s} * \boldsymbol{x}) * (\boldsymbol{\delta}_s * \boldsymbol{h})$	centered PSF $\alpha_1 = \alpha_2 = 0$ (tip-tilt)
– identity	$\boldsymbol{\delta} * \boldsymbol{y} = \boldsymbol{y}$	limited bandwidth: $\boldsymbol{h} \neq \boldsymbol{\delta}$
– reducibility	$(\boldsymbol{g} * \boldsymbol{x}) * \boldsymbol{h} = \boldsymbol{x} * (\boldsymbol{g} * \boldsymbol{h})$	empirical evidence
– inversion	$\boldsymbol{x} * \boldsymbol{h} = (\boldsymbol{s} * \boldsymbol{x}) * \left(\boldsymbol{s}^{-1} * \boldsymbol{h}\right)$	empirical evidence

The proposed parameterization solves classical blind deconvolution degeneracies.

Suppression of degeneracies

Degeneracies of blind deconvolution:

– permutation	$\boldsymbol{x} * \boldsymbol{h} = \boldsymbol{h} * \boldsymbol{x}$	object $\neq$ diffraction pattern
– scaling	$(\alpha\, \boldsymbol{x}) * \boldsymbol{h} = \boldsymbol{x} * \left(\frac{1}{\alpha}\boldsymbol{h}\right)$	normalized PSF: $\sum_n \beta_n^2 = 1$
– shift	$\boldsymbol{x} * \boldsymbol{h} = (\boldsymbol{\delta}_{-s} * \boldsymbol{x}) * (\boldsymbol{\delta}_s * \boldsymbol{h})$	centered PSF $\alpha_1 = \alpha_2 = 0$ (tip-tilt)
– identity	$\boldsymbol{\delta} * \boldsymbol{y} = \boldsymbol{y}$	limited bandwidth: $\boldsymbol{h} \neq \boldsymbol{\delta}$
– reducibility	$(\boldsymbol{g} * \boldsymbol{x}) * \boldsymbol{h} = \boldsymbol{x} * (\boldsymbol{g} * \boldsymbol{h})$	empirical evidence
– inversion	$\boldsymbol{x} * \boldsymbol{h} = (\boldsymbol{s} * \boldsymbol{x}) * \left(\boldsymbol{s}^{-1} * \boldsymbol{h}\right)$	empirical evidence

The proposed parameterization solves classical blind deconvolution degeneracies.

Suppression of degeneracies

Degeneracies of blind deconvolution:

– permutation	$\boldsymbol{x} * \boldsymbol{h} = \boldsymbol{h} * \boldsymbol{x}$	object $\neq$ diffraction pattern
– scaling	$(\alpha\, \boldsymbol{x}) * \boldsymbol{h} = \boldsymbol{x} * \left(\frac{1}{\alpha}\boldsymbol{h}\right)$	normalized PSF: $\sum_n \beta_n^2 = 1$
– shift	$\boldsymbol{x} * \boldsymbol{h} = (\boldsymbol{\delta}_{-s} * \boldsymbol{x}) * (\boldsymbol{\delta}_s * \boldsymbol{h})$	centered PSF $\alpha_1 = \alpha_2 = 0$ (tip-tilt)
– identity	$\boldsymbol{\delta} * \boldsymbol{y} = \boldsymbol{y}$	limited bandwidth: $\boldsymbol{h} \neq \boldsymbol{\delta}$
– reducibility	$(\boldsymbol{g} * \boldsymbol{x}) * \boldsymbol{h} = \boldsymbol{x} * (\boldsymbol{g} * \boldsymbol{h})$	empirical evidence
– inversion	$\boldsymbol{x} * \boldsymbol{h} = (\boldsymbol{s} * \boldsymbol{x}) * \left(\boldsymbol{s}^{-1} * \boldsymbol{h}\right)$	empirical evidence

The proposed parameterization solves classical blind deconvolution degeneracies.

Suppression of degeneracies

Degeneracies of blind deconvolution:

– permutation	$\boldsymbol{x} * \boldsymbol{h} = \boldsymbol{h} * \boldsymbol{x}$	object $\neq$ diffraction pattern
– scaling	$(\alpha\, \boldsymbol{x}) * \boldsymbol{h} = \boldsymbol{x} * \left(\frac{1}{\alpha}\boldsymbol{h}\right)$	normalized PSF: $\sum_n \beta_n^2 = 1$
– shift	$\boldsymbol{x} * \boldsymbol{h} = (\boldsymbol{\delta}_{-s} * \boldsymbol{x}) * (\boldsymbol{\delta}_s * \boldsymbol{h})$	centered PSF $\alpha_1 = \alpha_2 = 0$ (tip-tilt)
– identity	$\boldsymbol{\delta} * \boldsymbol{y} = \boldsymbol{y}$	limited bandwidth: $\boldsymbol{h} \neq \boldsymbol{\delta}$
– reducibility	$(\boldsymbol{g} * \boldsymbol{x}) * \boldsymbol{h} = \boldsymbol{x} * (\boldsymbol{g} * \boldsymbol{h})$	empirical evidence
– inversion	$\boldsymbol{x} * \boldsymbol{h} = (\boldsymbol{s} * \boldsymbol{x}) * \left(\boldsymbol{s}^{-1} * \boldsymbol{h}\right)$	empirical evidence

The proposed parameterization solves classical blind deconvolution degeneracies.

Blind deconvolution algorithm

$$\{\boldsymbol{f}^+, n_i^+, \boldsymbol{\alpha}^+, \boldsymbol{\beta}^+, \boldsymbol{\delta}^+\} = \underset{\boldsymbol{f}, n_i, \boldsymbol{\alpha}, \boldsymbol{\beta}}{\arg\min} \left\{ \mathcal{J}_{\text{data}}(\boldsymbol{f}, \boldsymbol{h}(n_i, \boldsymbol{\alpha}, \boldsymbol{\beta}, \boldsymbol{\delta}; \boldsymbol{g})) + \mu \mathcal{J}_{\text{prior}}(\boldsymbol{f}) \right\}$$

Non-convex and ill-conditionned problem solved by alternated minimization

- $t = 0$, start with the diffraction-limited PSF $h^{(0)}$ ($\alpha = \beta = 0$),
  1. $t = t + 1$, estimation of the optimal non-negative object $\boldsymbol{f}^{(t)}$ with given PSF $\boldsymbol{h}^{(t-1)}$:
     $\boldsymbol{f}^{(t)} \approx \arg\min_{\boldsymbol{f} \geq 0} \left(\mathcal{J}_{\text{data}}(\boldsymbol{f}, \boldsymbol{h}^{(t-1)}) + \mu \mathcal{J}_{\text{prior}}(\boldsymbol{f}) \right)$,
  2. Estimation of defocus parameters:
     $\{k_0^{(t)}, \boldsymbol{\delta}^{(t)}\} = \arg\min_{\{k_i, \boldsymbol{\delta}\}} \mathcal{J}_{\text{data}} \left(\boldsymbol{f}^{(t)}, \boldsymbol{h}(\alpha^{(t-1)}, \beta^{(t-1)}, k_0, \boldsymbol{\delta}) \right)$.
  3. Estimation of phase parameters:
     $\alpha^{(t)} = \arg\min_{\alpha} \mathcal{J}_{\text{data}} \left(\boldsymbol{f}^{(t)}, \boldsymbol{h}(\alpha, \beta^{(t-1)}, k_0^{(t)}, \boldsymbol{\delta}^{(t)}) \right)$.
  4. Estimation of module parameters:
     $\beta^{(t)} = \arg\min_{\sum \beta^2 = 1} \mathcal{J}_{\text{data}} \left(\boldsymbol{f}^{(t)}, \boldsymbol{h}(\alpha^{(t)}, \beta, k_0^{(t)}, \boldsymbol{\delta}^{(t)}) \right)$,
- until convergence.

Blind deconvolution algorithm

$$\{\boldsymbol{f}^+, n_i^+, \boldsymbol{\alpha}^+, \boldsymbol{\beta}^+, \boldsymbol{\delta}^+\} = \arg\min_{\boldsymbol{f}, n_i, \boldsymbol{\alpha}, \boldsymbol{\beta}} \left\{ \mathcal{J}_{\text{data}}(\boldsymbol{f}, \boldsymbol{h}(n_i, \boldsymbol{\alpha}, \boldsymbol{\beta}, \boldsymbol{\delta}; \boldsymbol{g})) + \mu \mathcal{J}_{\text{prior}}(\boldsymbol{f}) \right\}$$

Non-convex and ill-conditionned problem solved by alternated minimization

- $t = 0$, start with the diffraction-limited PSF $h^{(0)}$ ($\boldsymbol{\alpha} = \boldsymbol{\beta} = 0$),
  1. $t = t + 1$, estimation of the optimal non-negative object $\boldsymbol{f}^{(t)}$ with given PSF $\boldsymbol{h}^{(t-1)}$:
     $\boldsymbol{f}^{(t)} \approx \arg\min_{\boldsymbol{f} \geq 0} \left(\mathcal{J}_{\text{data}}(\boldsymbol{f}, \boldsymbol{h}^{(t-1)}) + \mu \mathcal{J}_{\text{prior}}(\boldsymbol{f}) \right)$,
  2. Estimation of defocus parameters:
     $\{k_0^{(t)}, \boldsymbol{\delta}^{(t)}\} = \arg\min_{\{k_i, \boldsymbol{\delta}\}} \mathcal{J}_{\text{data}} \left(\boldsymbol{f}^{(t)}, \boldsymbol{h}(\boldsymbol{\alpha}^{(t-1)}, \boldsymbol{\beta}^{(t-1)}, k_0, \boldsymbol{\delta}) \right)$.
  3. Estimation of phase parameters:
     $\boldsymbol{\alpha}^{(t)} = \arg\min_{\boldsymbol{\alpha}} \mathcal{J}_{\text{data}} \left(\boldsymbol{f}^{(t)}, \boldsymbol{h}(\boldsymbol{\alpha}, \boldsymbol{\beta}^{(t-1)}, k_0^{(t)}, \boldsymbol{\delta}^{(t)}) \right)$.
  4. Estimation of module parameters:
     $\boldsymbol{\beta}^{(t)} = \arg\min_{\sum \beta^2 = 1} \mathcal{J}_{\text{data}} \left(\boldsymbol{f}^{(t)}, \boldsymbol{h}(\boldsymbol{\alpha}^{(t)}, \boldsymbol{\beta}, k_0^{(t)}, \boldsymbol{\delta}^{(t)}) \right)$,
- until convergence.

Simulations

Comparison of several methods from [Kenig,2010]:

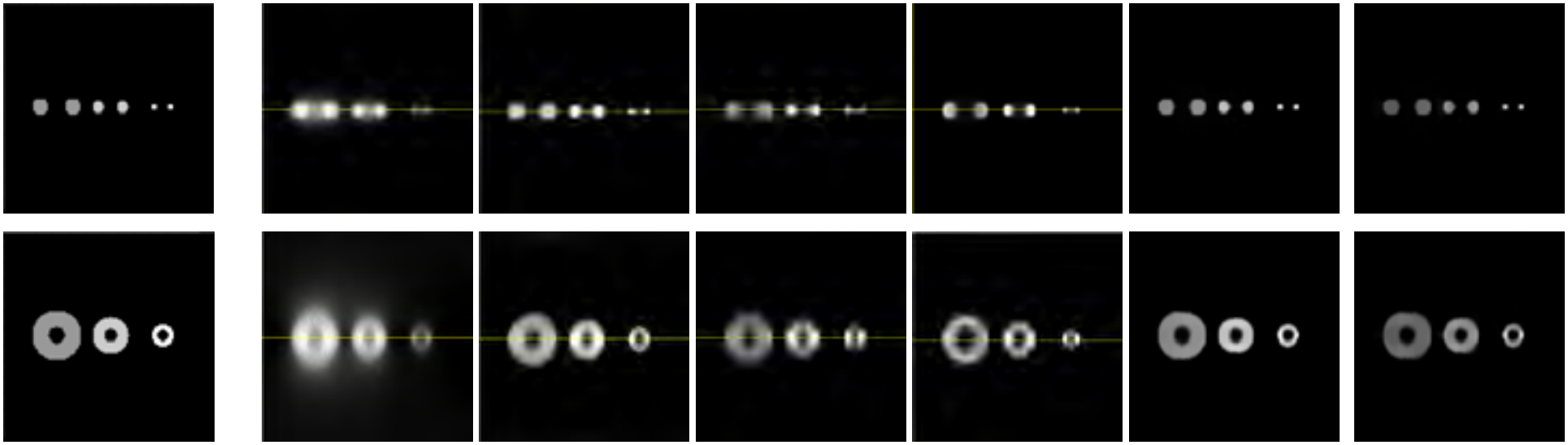

MSE =	35.81	25.47	19.30	19.10	9.59	10.55
(a) ground truth	(b) data	(c) AIDA	(d) KPCA	(e) Keuper	(f) **dec.**	(g) **bl. dec.**

AIDA: [Hom,2007], KPCA: [Kenig,2010], Keuper: [Keuper,2013]

Experimental results: calibration beads

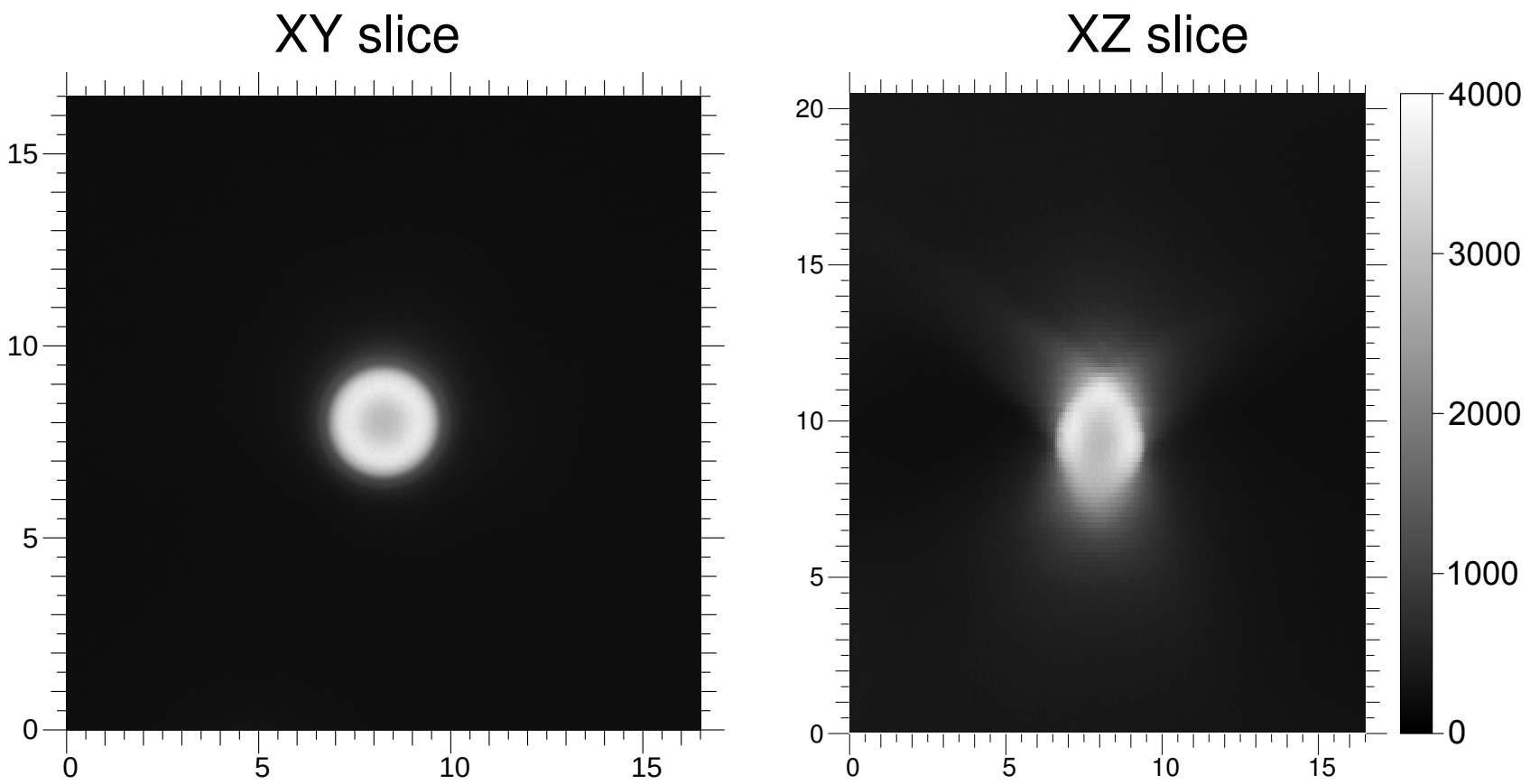

— Diameter: 2.5μm, $\mathrm{NA} = 1.4$
— 256^3 pixels $64.5 \times 64.5 \times 160\mathrm{nm}^3$
data from [Griffa,2010]

Deconvolution with the theoretical PSF

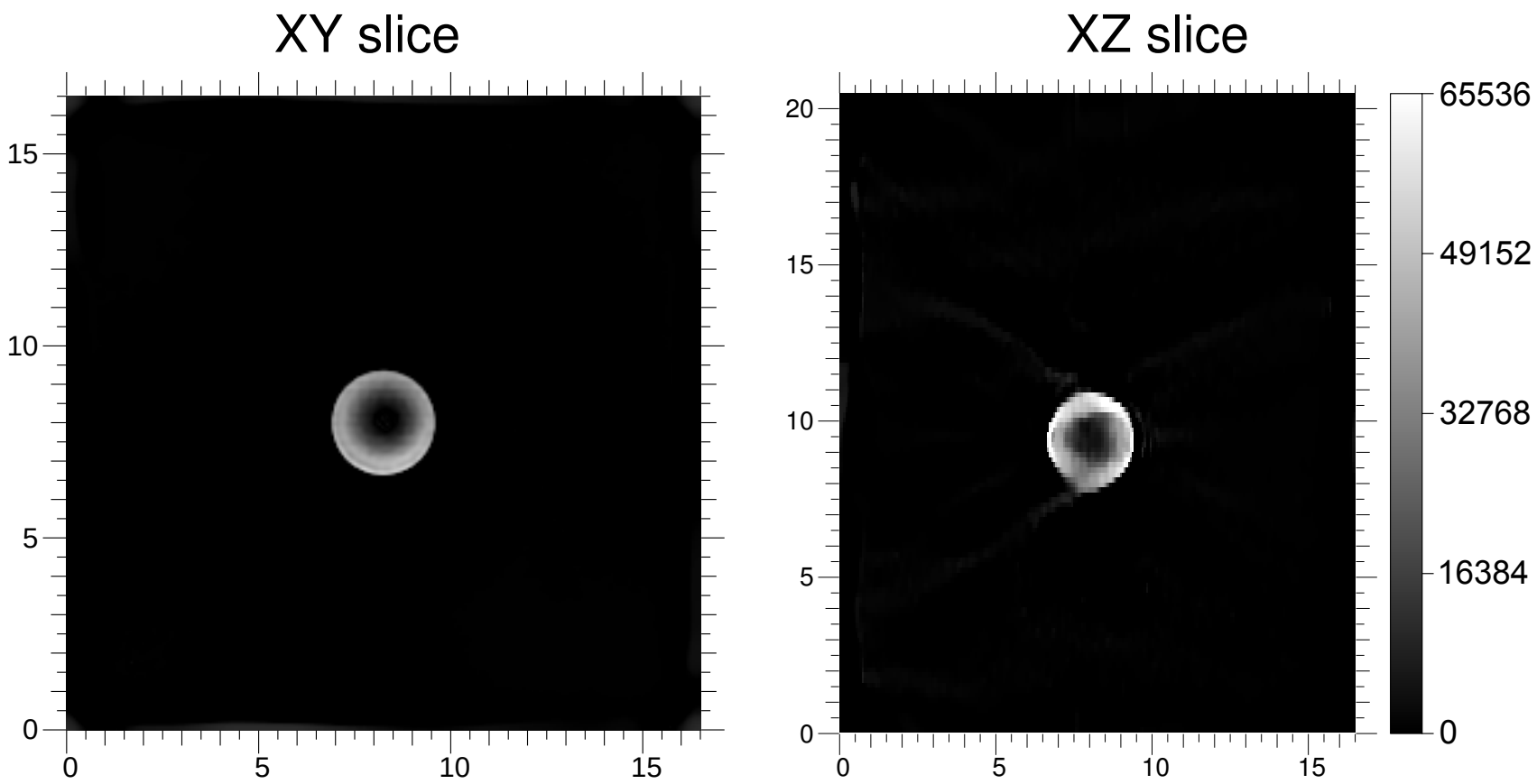

— Diameter: 2.5μm, $\mathrm{NA} = 1.4$
— 256^3 pixels $64.5 \times 64.5 \times 160\mathrm{nm}^3$
data from [Griffa,2010]

Blind deconvolution

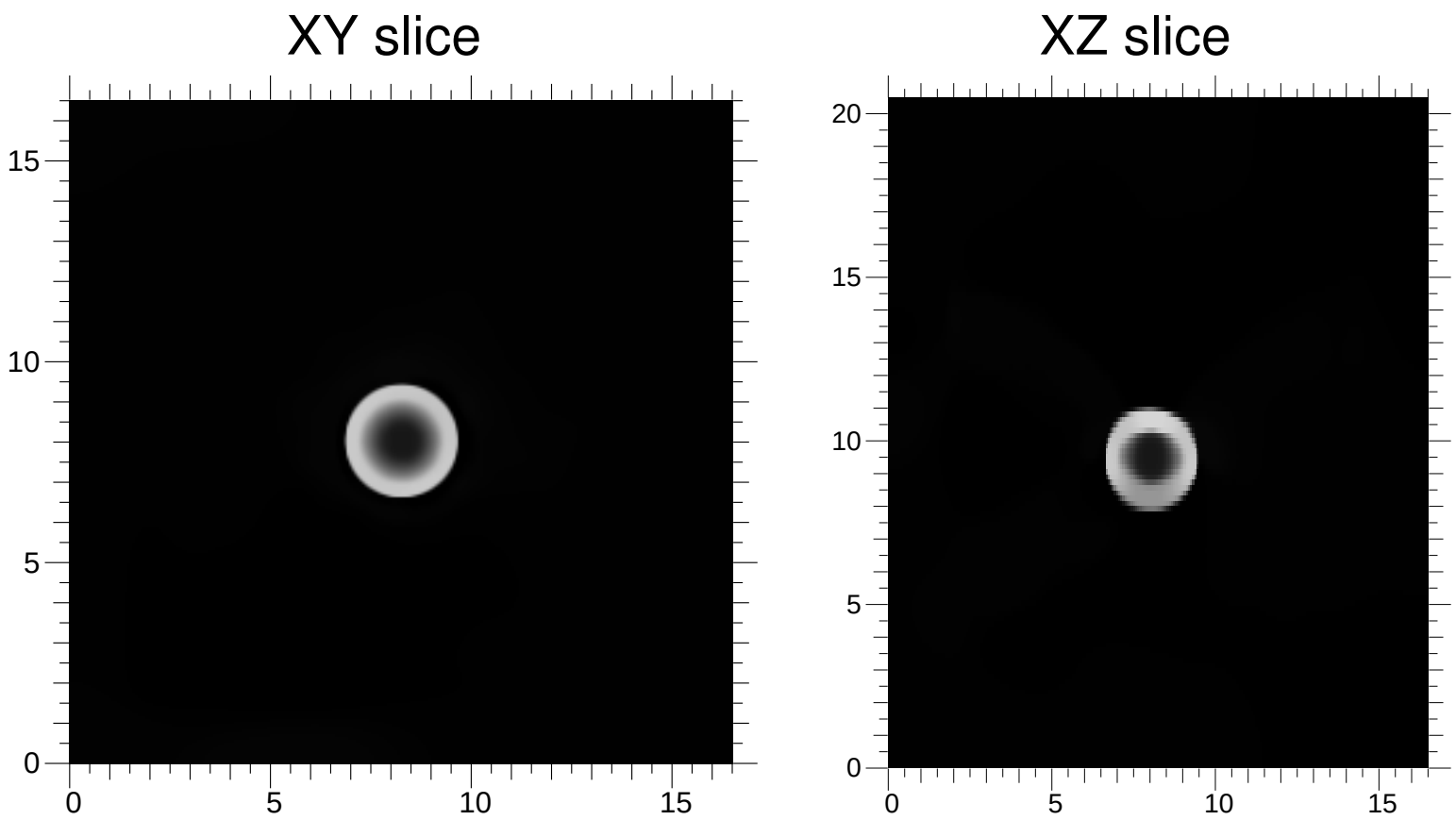

— Diameter: 2.5μm, $\mathrm{NA} = 1.4$
— 256^3 pixels $64.5 \times 64.5 \times 160\mathrm{nm}^3$
data from [Griffa,2010]

Calibration beads

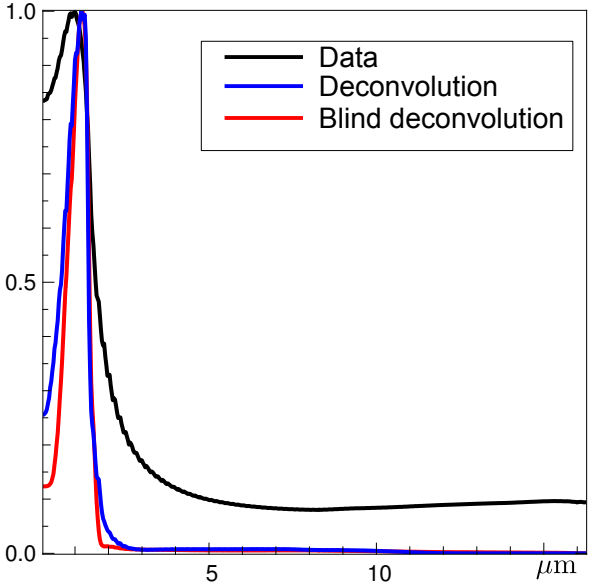

3D radial profile of the bead

parameters	data	Hyugens	AutoDeblur	Deconvol. Lab	proposed method non blind.	proposed method blind
transversal FWHM	2.87	2.71	2.71	**2.66**	2.74	2.78
axial FWHM (en μm)	4.76	4.00	4.64	4.16	3.05	**2.98**
relative contrast	18 %	53 %	78 %	68 %	84 %	**88** %

Performance of 3 deconvolution methods from [Griffa,2010], compared with our method.

Hyugens et AutoDeblur are commercial software Deconvolution Lab is a plugin for imageJ

Calibration beads: PSF

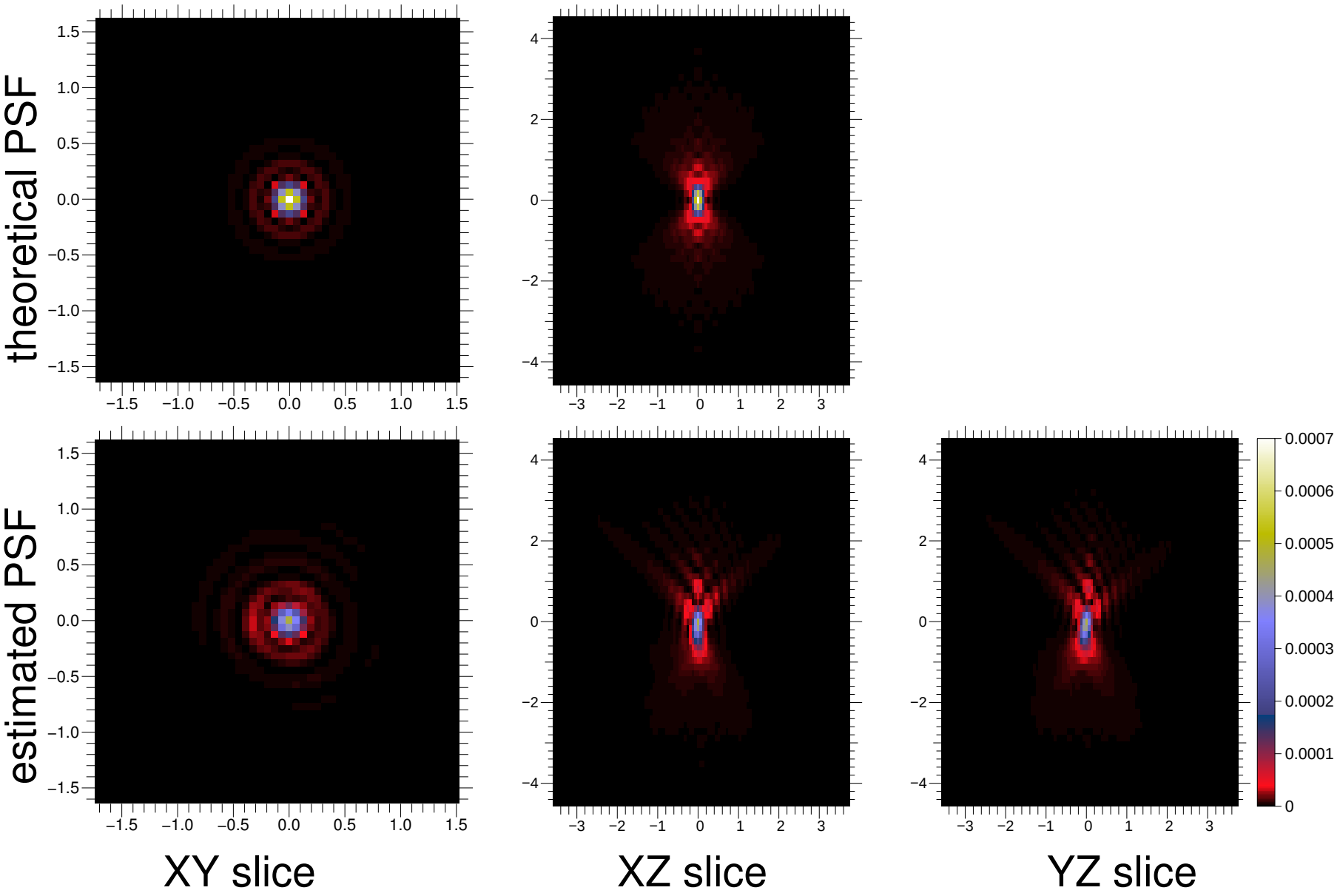

Experimental data

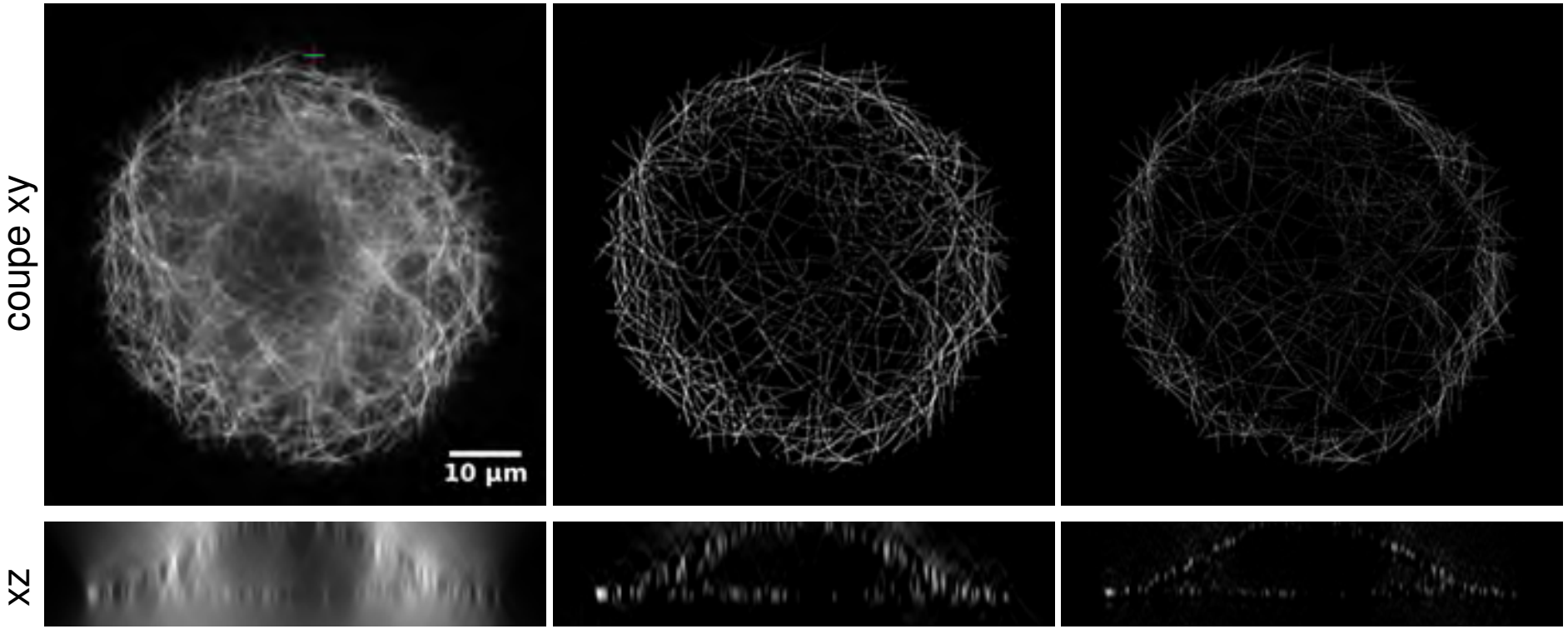

(a) data (b) blind deconv. (c) SIM

Blind deconvolution of S2 cell compared to wide field and structured illumination microscopy.

$(1024 \times 1024 \times 44)$ voxels of $40 \times 40 \times 110\,\mathrm{nm}^3$. $\mathrm{NA} = 1.4$.

Experimental data

xy slice and xz slice of a filament:

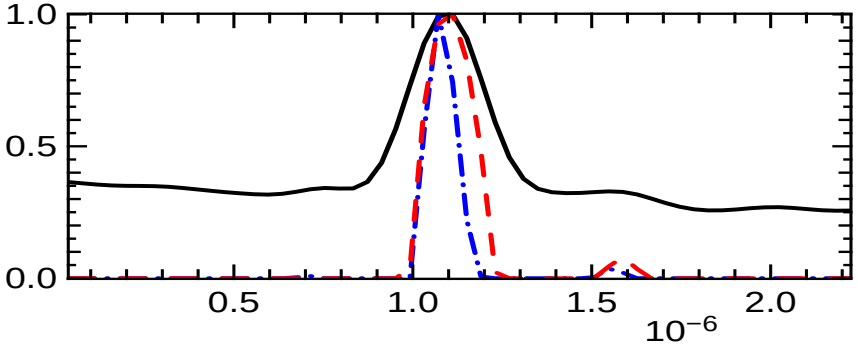

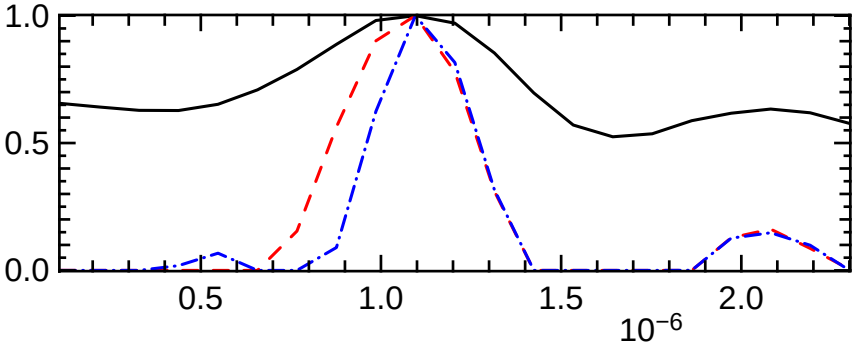

xy slice — data - - blind deconvolution

xz slice - - SIM

Resolution close to that of a structured illumination microscope (SIM) with a simple wide field microscope!

Experimental data: C. Elegans

Embryon de C. Elegans

- microscope lens $\times 63$, $1.4\ \mathrm{NA}$,
- $672 \times 712 \times 104$ voxels,
- voxels $64.5 \times 64.5 \times 200\ \mathrm{nm}^3$

data from [Griffa,2010]